

Optimal sizing of a holdout set for safe predictive model updating

Sami Haidar-Wehbe^{1,†}, Samuel R. Emerson^{1,†},
Louis J. M. Aslett^{1,2}, James Liley¹

1: Department of Mathematical Sciences, Durham University, Durham, UK; 2: Alan Turing Institute, London, UK; †: Equal contribution
Correspondence to {louis.aslett, james.liley}@durham.ac.uk

February 18, 2022

Abstract

Risk models in medical statistics and healthcare machine learning are increasingly used to guide clinical or other interventions. Should a model be updated after a guided intervention, it may lead to its own failure at making accurate predictions. The use of a ‘holdout set’ – a subset of the population that does not receive interventions guided by the model – has been proposed to prevent this. Since patients in the holdout set do not benefit from risk predictions, the chosen size must trade off maximising model performance whilst minimising the number of held out patients. By defining a general loss function, we prove the existence and uniqueness of an optimal holdout set size, and introduce parametric and semi-parametric algorithms for its estimation. We demonstrate their use on a recent risk score for pre-eclampsia. Based on these results, we argue that a holdout set is a safe, viable and easily implemented solution to the model update problem. Model update; Machine learning safety; Machine learning in healthcare; Predictive model; Holdout set; Treatment decision

1 Introduction

Risk scores estimate the probability of an event Y given predictors X . Their use has become routine in medical practice (Topol, 2019), where Y may represent disease incidence and X various clinical observations. Once calculated, risk scores may be used to guide interventions (perhaps modifying X), with the aim of decreasing the probability of an adverse Y . For example, the QRISK3 score predicts thromboembolic risk given predictors including age and hypertension (Hippisley-Cox et al., 2017), and a high score may prompt prescription of antihypertensives.

Risk scores are typically developed by regressing observations of Y on X . Should the distribution of (X, Y) subsequently change (or ‘drift’), then risk estimates may become biased (Tsymbal, 2004; Zliobaite, 2010). This can happen naturally over time, meaning that risk scores typically need to be updated periodically to maintain their utility.

Updating of the risk score will involve obtaining new observations of (X, Y) . Crucially the distribution of (X, Y) may also change due to the effect of the risk score itself: that is, high predicted risk of an adverse event may trigger intervention to reduce that risk. The effect of such interventions may be difficult to infer, and indeed the act of intervening is often unrecorded. In the QRISK3 example above, individuals prescribed antihypertensives in response to higher QRISK3 scores should have lower thromboembolic risk than they would have if QRISK3 was not used. Should a new risk score be fitted to observed (X, Y) , the effect of hypertension on risk would be underestimated, and overall risk estimates upwards-biased. This bias is worsened by heavier intervention resulting in risk scores becoming ‘victims of their own success’ (Lenert et al., 2019). This framework of directly updating a risk score on an ‘intervened’ population has been termed ‘repeated risk minimisation’ (Perdomo et al., 2020) or ‘naïve updating’ (Liley et al., 2021b).

A possible solution to this problem is to split the population on which the score can be used into an ‘intervention’ set and a ‘holdout’ set (Liley et al., 2021b). Risk scores are computed for samples in the intervention set and allowed to guide intervention, while risk scores are not computed for samples in the holdout set. As opposed to naïve model updating, we now update the model using data exclusively from samples in the holdout set. This allows the model to be updated safely, since only natural drift is represented in the holdout set. This poses a vital tension, the resolution of which is the primary contribution of this paper: for the risk score to be accurate, the holdout set should not be too small; but, any samples in the holdout set will not benefit from risk scores, so nor should it be too large. In this work we develop methodology to ascertain the optimal size for a holdout set which balances these conflicting goals.

Contributions in this area are important due to rapidly evolving legislation. Currently, the European Union treat each update of a risk model as a separate risk score requiring re-approval, but in the USA a proactive approach is taken with a ‘total-life cycle’ paradigm which allows practitioners to update risk models as necessary without requesting approval (USFDA et al., 2019). This approach could allow updating-induced biases to go undetected, and highlights the need for safe updating methods in risk score deployment. The use of holdout sets as examined in this work offers one potential solution.

Our paper is structured in the following way. In Section 2, we review relevant literature and precisely define the problem. In Section 3, we quantify the expected cost as a function of holdout set size, and describe reasonable sufficient conditions under which an Optimal Holdout set Size (OHS) exists. In Section 4, we then describe two algorithms for OHS estimation, together with supporting theory: the first using an explicit parametrisation; the second using Bayesian emulation to allow deviation from these parametric assumptions. In Section 5, we support our findings with numerical demonstrations and apply our algorithms

to a risk score for pre-eclampsia (PRE) to estimate an OHS for updating it.

2 Review of related work

Widespread collection of electronic health records has spurred development of new diagnostic and prognostic risk scores (Cook and Collins, 2015; Liley et al., 2021a), which can allow detection of patterns too complex for humans to discover (Koopman and Mainous, 2008). Examples of such scores in widespread use include: EuroSCORE II, which predicts mortality risk at hospital discharge following cardiac surgery (Nashef et al., 2012); and the STS risk score from the USA predicting risk of postoperative mortality (Jacobs et al., 2006; Shahian et al., 2018; O'Brien et al., 2018). Many such scores have demonstrable efficacy in clinical trials and in-vivo (Ad et al., 2016; Chalmers et al., 2013; Barili et al., 2013; Wallace et al., 2014; Durand et al., 2013).

An important general concern with these scores is continued accuracy of predictions. A 2011 review, found that risk scores for hospital readmission perform poorly and highlighted issues with design of their trials (Kansagara et al., 2011). More recently, an analysis of a sepsis response score used during the COVID pandemic found increasing risk overestimation over time Finlayson et al. (2020). Various efforts have been made to standardise procedures in risk score estimation to address these issues Collins et al. (2015, 2021).

Several algorithms have been developed to update models with new data in the presence of drift (Lu et al., 2018), which ideally leads to the best possible model performance after every update. Adaptation of model updating to avoid naïve updating-induced bias requires explicit causal reasoning (Sperrin et al., 2019) and often further data collection (Liley, 2021). In a seminal paper, Perdomo et al. (2020) analyse asymptotic behaviour of repeated naïve updating, giving necessary and sufficient conditions for successive predictions to converge to a stable setting where they ‘predict their own effect’. Other approaches to optimise a general loss function by modulating parameters of the risk score are developed in Mendler-Dünner et al. (2020); Drusvyatskiy and Xiao (2020); Li and Wai (2021) and Izzo et al. (2021). These approaches seek to minimise a ‘performatice’ loss to the population in the presence of an arbitrary risk score. Our alternative approach seeks to target risk scores which reliably estimate the same quantity, namely $pr(Y | X)$ in a ‘native’ system prior to risk score deployment. Our approach is well-suited to settings where the performative loss is essentially intractable, requiring cost estimates of risk scores only in limited settings. We note ‘stability’ is not necessarily desirable in terms of distribution of interventions: in the QRISK3 setting, if an individual is at untreated risk of 50% and treated risk of 10%, with treatment distributed proportionally to assessed risk, a ‘stable’ risk score would assess risk as e.g. 30%, prompting a mild intervention after which true risk remained at 30%, regardless of treatment cost.

We found no literature directly addressing the focus in this paper: determining how large a holdout set should be. Similar problems do arise in clinical trial design. For

example, Stallard et al. (2017) describe a method to estimate the optimal size of clinical trial groups for a rare disease in which individuals not in the trial stand to gain more than those in it. A Bayesian decision-theoretic method is used to optimise a gain function while accounting for benefit to future patients in the population.

OHS estimation requires quantification of expected material costs when using risk scores trained to data of various sizes. Such costs will typically depend on the error of risk predictions. The relation of predictive error to training set size is known as the ‘learning curve’, which can sometimes be accurately parametrised (Amari et al., 1992; Amari, 1993). A recent review paper suggests a power-law is accurate for simple models (Viering and Loog, 2021).

3 Theory

3.1 General setup

Our general strategy for safe model updating using a hold-out set is illustrated in Figure 1, which is interpretable as a causal graph. Each of the three columns is called an ‘epoch’ (0,1,2 in subscripts), representing a period of time in which a risk score is deployed and data gathered to construct such a risk score. Ellipses containing X or Y are covariates and outcomes (respectively) of populations of samples. Under a ‘native’ setting prior to deployment of a risk score, X_0 and Y_0 have a single causal link, modelled by risk score ρ_0 (leftmost epoch). Once ρ_0 is in use in the intervention set in epoch 1 (ellipses X_1^i , Y_1^i), a second causal pathway through ρ_0 is established from X_1^i to Y_1^i , but there remains only one causal pathway from X_1^h to Y_1^h in the holdout set (middle epoch). The updating process can be continued rightwards (ρ_1 , ρ_2 , …).

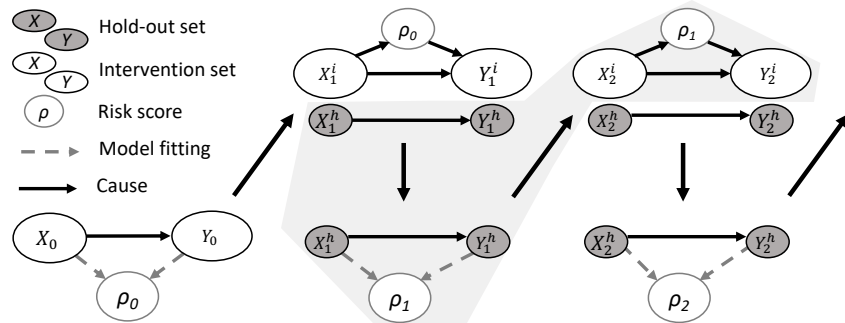


Figure 1: Dynamics of a risk model across epochs when trained on a holdout set.

In each epoch e a new risk score ρ_e is trained. A model is only ever used to make predictions on the same system to which it was trained (under a naïve updating setting,

this is not the case; ρ_1 would be trained to the system X_1^i, Y_1^i linked through ρ_0 , and used on a system X_2^i, Y_2^i in which they are not).

Because the variables inside the grey region are independent of those outside it, we may consider them in isolation. For notational convenience, we jointly consider samples in the holdout set in epoch e and in the intervention set in epoch $e+1$, and will assume that the total population size and holdout set size is the same across all epochs.

3.2 Notation

Suppose the aggregate groups above comprise n holdout set samples D_n which are independent and identically distributed as (X_e^h, Y_e^h) , and N samples in total, where the remaining $N - n$ samples in the intervention set are independent and identically distributed as (X_{e+1}^i, Y_{e+1}^i) . A risk score is fitted to the holdout set which approximates $\mathbb{E}(Y_e^h | X_e^h = x)$ and is used in the intervention set, affecting $Y_{e+1}^i | X_{e+1}^i$. We denote the standard normal PDF and CDF by $\phi(\cdot)$, $\Phi(\cdot)$ respectively.

We presume that we fit a risk score to D_n for use in epoch $e+1$. We define $C_1(X)$ and $C_2(X; D_n)$ as random variables associated with the total ‘cost’ of an observation with covariates X in the holdout set in epoch e and intervention set in epoch $e+1$ respectively, where the cost covers both the cost of managing the event $Y = 1$, as well as any gains or losses associated with intervention. Function $C_2(X; D_n)$ depends on D_n only through the fitted risk score.

We define the expected cost per observation in the holdout and intervention sets, respectively, as

$$\begin{aligned} k_1 &= \mathbb{E}_{X \sim X_e^h, C_1} \{C_1(X)\} \\ k_2(n) &= \mathbb{E}_{X \sim X_{e+1}^i, C_2} \{\mathbb{E}_{D_n} [C_2(X; D_n)]\} \end{aligned} \quad (1)$$

recalling that $D_n \sim (X_e^h, Y_e^h)^n$. Values C_1 and C_2 in outer expectations encompass variance in $C_1(X)$, $C_2(X; D_n)$ independent of X, D_n .

3.3 Sufficient conditions for optimal holdout size

We make the following assumptions, and describe their interpretation in a hypothetical medical context similar to QRISK3 (Hippisley-Cox et al., 2017).

1. k_1 does not depend on n : treatment plans and outcomes for patients without risk scores do not depend on the number of such patients.
2. $k_2(n)$ is monotonically decreasing in n : the more data available to train the risk score, the greater its clinical utility.
3. There exists an M with $0 < M < N$ such that $n \geq M \Leftrightarrow k_1 < k_2(n)$: a good enough risk score will lead to better patient outcomes than baseline treatment, and a poor

enough risk score fitted to small amounts of data leads to worse expected outcomes than baseline.

4. $\mathbb{E}[k_2(i+1) - k_2(i)] > \mathbb{E}[k_2(j+1) - k_2(j)]$ for $1 \leq i < j \leq N-1$: the ‘learning curve’ for our risk score is convex; there are diminishing returns in the cost per patient from adding more samples to the training data.

We now express total cost, ℓ , across the sample population as

$$\begin{aligned} \ell(n) &= k_1 n && \text{(tot. cost. holdout set)} \\ &+ k_2(n)(N - n) && \text{(tot. cost. intervention set)} \end{aligned}$$

We may freely extend the domain of $k_2(\cdot)$, $\ell(\cdot)$ to the real interval $[0, N]$ in such a way that both functions are smooth; and $k_2'(n) < 0$ (given assumption 2), $k_2''(n) > 0$ (given assumption 4).

This leads to the first core result, namely that there does indeed exist an optimal size for the holdout set which minimises the expected total cost. The proof is given in Appendix A1.

Theorem 1. *Suppose assumptions 1-4 hold. Then there exists an $N_* \in \{1, \dots, N-1\}$ with $N \in \mathbb{N}$, such that:*

$$\begin{aligned} \ell(i) &\geq \ell(j) \text{ for } 0 < i < j < N_* \\ \ell(i) &\leq \ell(j) \text{ for } N_* < i < j < N \end{aligned}$$

We refer to N_* as the *optimal holdout set size*.

The following Corollary is an immediate consequence: that the optimal holdout set size always exceeds the minimal training sample size required to match baseline treatment.

Corollary 1.1. *The value of N_* always exceeds the value of M in assumption 3, since if $N' < M$ we have*

$$\ell(N') = k_1 N' + k_2(N')(N - N') > k_1 N' + k_1(N - N') = k_1 N \geq \ell(N_*)$$

Consequently assumption 4 may be relaxed for $i, j < M$ (though to avoid tedious details we will generally not do so in this work); in other words, we need only be concerned with the behaviour of $k_2(n)$ at realistically large values of n , rather than $n \in 1, 2, \dots, M$.

We also note that

$$\lim_{N \rightarrow \infty} \lim_{n \rightarrow N} \ell'(n) = \lim_{N \rightarrow \infty} \lim_{n \rightarrow N} (k_1 - k_2(n) + (N - n)k_2'(n)) = k_1 - \lim_{n \rightarrow \infty} k_2(n) \quad (2)$$

and since $k_1 > k_2(n) > 0$ for large n , we have that expected total costs are increasing, but bounded by the per observation expected cost of baseline treatment k_1 .

4 Estimation of Optimal Holdout Set Size (OHS)

4.1 Practicalities

In order to estimate the OHS, we must estimate the cost function $\ell(n)$ up to a linear transformation, which in turn entails estimating the constants N , k_1 , and the function k_2 .

Such estimates may be made in several ways. A simple option may be to use expert opinion or literature search, and in some cases it may be possible to compute expected cost directly, especially if the action taken on a risk score is systematically determined, as may be the case for medical risk scores (Williams, 2003). A more general option is to use some mechanism to estimate the cost dependence on holdout set sizes, via pairs $(n, C_2(n))$, $(n, k_2(n))$ or $(n, \ell(n))$. Even if such point estimates are not made directly, we will assume in our parametric method (section 4.2) that errors in estimates of N , k_1 , k_2 decrease as the inverse square root of effort made to measure them; that is, behave as though dependent on some number of such point estimates, in that estimates may be made more accurate at a tradeoff of greater cost. If, for instance, an expert opinion poll is used, then more or fewer opinions may be collected.

A gold-standard option to make an unbiased estimate of $(n, k_2(n))$ is through an interventional trial, in which a cohort of individuals are given risk scores fitted to a set amount of training data (several scores may be tested on sample subcohorts in parallel), the eventual cost C_2 measured directly, and these regressed to the expected cost (possibly with constraints to observe assumptions 1–4). Although such trials could potentially be conducted at the time an initial risk score is fitted, this option may not be necessary.

It may be reasonable to assume that C_2 (and hence k_2) is a linear function $\mathcal{L}(\cdot)$ of some measure of the predictive accuracy of the risk score (e.g., mean mis-classification error), and work with this predictive accuracy $\mathcal{L}^{-1}(k_2)$ instead, since $\mathcal{L}^{-1}(\ell)$ will conserve the OHS of ℓ . We demonstrate an example in section 5.3. This assumption necessitates an estimate of $\mathcal{L}^{-1}(k_1)$ (the ‘accuracy of no risk score’), which is typically straightforward and results in an overall simplification of the estimation problem, since \mathcal{L} need never be made explicit. That is, only the expected predictive accuracy of the score at candidate holdout set sizes n need to be calculated, which can be achieved readily using training observations of X and Y when no score is in use.

In the following sections, we will consider that observation/estimation of points $(n, k_2(n))$ may be costly and seek to minimise the number of such pairs that must be used. We consider that the constants N (the total number of samples on which a given predictive score can be fitted or used) and k_1 (the average cost per sample under baseline behaviour without a score) will generally be possible to estimate, although we still allow for error in their estimation.

4.2 Parametric estimation of OHS

A natural algorithm for estimating the optimal holdout set size (OHS), should it exist, is immediately suggested by Theorem 1: assume k_2 is known up to parameters θ , and estimate N , k_1 and θ to estimate the optimal holdout size.

Parameters θ of k_2 may be estimated from observations of pairs $(n, k_2(n))$, potentially with error in $k_2(n)$. To minimise the number of times we have to estimate $k_2(n)$ we suggest iteratively adding observations n to an existing set of estimation data in such a way as to greedily reduce the expected error in the resultant OHS estimate.

We firstly develop asymptotic confidence intervals for parametric OHS estimates to link error in parameter estimates to error in OHS. We will take k'_2 , k''_2 , ℓ' to mean partial derivatives with respect to n . If for θ in some neighbourhood of its true value we have

$$k'_2(n; \theta) < 0 \quad \text{and} \quad k''_2(n; \theta) > 0 \quad (3)$$

and hence

$$\ell''(n; \theta) = (N - n)k''_2(n; \theta) - 2k'_2(n; \theta) < 0 \quad (4)$$

then the function $\ell'(n; \theta)$ is continuous and monotonically increasing, and thus injective and invertible with respect to n . We may consider the optimal holdout set size N_* to be a rounding of a real solution n_* to $\ell'(n; \theta) = 0$, and in turn consider n_* as a real-valued function of θ , N , and k_1 (though not always defined). We then have

$$\begin{aligned} n_* &\triangleq \{n : \ell'(n; \theta) = 0\} \\ \frac{\partial n_*}{\partial \theta} &= \frac{\frac{\partial^2 \ell}{\partial n \partial \theta}}{\frac{\partial^2 \ell}{\partial n^2}} = -\frac{\frac{\partial}{\partial \theta}(-k_2(n; \theta) + k'_2(n; \theta)(N - n))}{(N - n)k''_2(n; \theta) - 2k'_2(n; \theta)} \\ \frac{\partial}{\partial \theta} \ell(n_*; \theta) &= \frac{\partial n_*}{\partial \theta} \ell'(n_*; \theta) + \frac{\partial \ell}{\partial \theta} = \frac{\partial \ell}{\partial \theta} \end{aligned} \quad (5)$$

and

$$\begin{aligned} \frac{\partial n_*}{\partial k_1} &= \frac{1}{(N - n)k''_2(n; \theta) - 2k'_2(n; \theta)} & \frac{\partial}{\partial k_1} \ell(n_*; \theta) &= n_* \\ \frac{\partial n_*}{\partial N} &= \frac{k'_2(n; \theta)}{(N - n)k''_2(n; \theta) - 2k'_2(n; \theta)} & \frac{\partial}{\partial N} \ell(n_*; \theta) &= k_2(n_*; \theta) \end{aligned}$$

We will use these expressions to construct asymptotic confidence intervals for n_* and $\ell(n_*)$ in the following Theorem. We will use the shorthand $\Theta = (N, k_1, \theta)$ and $\Theta_0 = \mathbb{E}(\Theta)$. We will also write $n_* = n_*(\Theta)$, $\ell(n_*) = \ell(n_*(\Theta); \Theta)$, $n_0 = n_*(\Theta_0)$ and $\ell(n_0) = \ell(n_*(\Theta_0), \Theta_0)$ for brevity. We presume that Θ is an unbiased estimate of parameters, so Θ_0 corresponds to ‘true’ parameter values. Note that the sample-size m used in the following Theorem denotes a proxy for effort expended in estimating Θ_0 , as will be expanded upon later.

Theorem 2. Assume that $k_2''(n; \theta)$, $k_2'(n; \theta)$ and $\nabla_\theta k_2(n; \theta)$ are continuous in n and θ in some neighbourhood of (n_0, Θ_0) , and that Θ_0 parametrises a setting satisfying assumptions 1-4. Suppose that Θ behaves as a mean of m appropriately-distributed samples in satisfying $\sqrt{m}(\Theta - \Theta_0) \rightarrow_d N(0, \Sigma)$ where Θ_0 does not depend on m , that an estimate $\hat{\Sigma}$ of Σ is available which is independent of Θ and satisfies $\|\hat{\Sigma} - \Sigma\|_2 \rightarrow_d 0$, and that n_0 is finite and unique as above. Then denoting

$$\beta_\Theta = \frac{\frac{\partial^2 \ell}{\partial n \partial \Theta_i}}{\frac{\partial^2 \ell}{\partial n^2}}, \quad \gamma_\Theta = \frac{\partial \ell}{\partial \Theta_i}$$

we may uniquely define $n_0 = \{n : \ell'(n; \Theta_0) = 0\}$ and we have

$$\sqrt{m}(n_* - n_0) \rightarrow_d N(0, \beta_{\Theta_0}^t \Sigma \beta_{\Theta_0}), \quad \sqrt{m}(\ell(n_*) - \ell(n_0)) \rightarrow_d N(0, \gamma_{\Theta_0}^t \Sigma \gamma_{\Theta_0})$$

and the confidence intervals

$$I_\alpha(\Theta, \hat{\Sigma}) = \left[n_*(\Theta) - z_\alpha \sqrt{\frac{\beta_\Theta^t \hat{\Sigma} \beta_\Theta}{m}}, n_*(\Theta) + z_\alpha \sqrt{\frac{\beta_\Theta^t \hat{\Sigma} \beta_\Theta}{m}} \right]$$

$$J_\alpha(\Theta, \hat{\Sigma}) = \left[\ell(n_*) - z_\alpha \sqrt{\frac{\gamma_\Theta^t \hat{\Sigma} \gamma_\Theta}{m}}, \ell(n_*) + z_\alpha \sqrt{\frac{\gamma_\Theta^t \hat{\Sigma} \gamma_\Theta}{m}} \right]$$

where $z_\alpha = \Phi^{-1}(1 - \frac{\alpha}{2})$, satisfy $P(n_0 \in I_\alpha(\Theta, \hat{\Sigma})) \rightarrow 1 - \alpha$ and $P(\ell(n_0) \in J_\alpha(\Theta, \hat{\Sigma})) \rightarrow 1 - \alpha$ as $m \rightarrow \infty$.

The proof of this Theorem is given in Appendix A2. A consequence is that for sufficiently accurately estimated costs, the OHS will be a non-trivial size as follows.

Corollary 2.1. Under the assumptions of Theorems 1 and 2, we have

$$P(1 < n_*(\Theta) < N) \rightarrow 1 \tag{6}$$

as $m \rightarrow \infty$.

In light of the proportionality assumption in Section 4.1, and the tendency of the accuracy of a risk score with number of training samples ('learning curve') to follow a power-law form (Viering and Loog, 2021), we recommend considering such a parametric form for k_2 (i.e. $k_2(n; \theta) = an^{-b} + c$ with $\theta = (a, b, c)$), and provide explicit asymptotic confidence intervals for this setting also in Appendix A2. Examples of variation in n_* and $\ell(n_*)$ with a power-law form for k_2 , are shown in supplementary figures 7, 8.

Note that confidence intervals must be interpreted with care: if the sampling distributions for k_1 and θ admit the possibility that assumptions of Theorem 1 are violated such that

$$P\left(k_1 < \liminf_{n \rightarrow \infty} \{k_2(n, \theta)\}\right) > 0 \tag{7}$$

then the standard error of n_* does not exist, as n_* can be undefined. Finite-sample confidence intervals may be constructed by bootstrapping (see function `ci_ohs()` in our R package `OptHoldoutSize`).

Our parametric algorithm assumes Θ is estimated from a multiset \mathbf{n} of values in $\{1, \dots, N\}$ and estimates \mathbf{d} of $k_2(n)$ for each $n \in \mathbf{n}$ with known finite sampling variances σ^2 . For certain multisets \mathbf{n} , estimates of Θ will not converge (for instance, if \mathbf{n} contains only a single value repeated), so m in Theorem 2 should be interpreted as an ‘effective’ population size, such that $\sqrt{m}(\Theta(\mathbf{n}) - \Theta_0) \rightarrow_d N(0, \Sigma)$.

Given that our eventual aim to estimate the OHS with minimal error, we suggest the following way to iteratively select a new value \tilde{n} at which an estimate $\hat{k}_2(\tilde{n})$ of $k_2(\tilde{n})$ should be made, given a set \mathbf{n} of points at which estimates \mathbf{k}_2 of $k_2(\mathbf{n})$ have been made already. We denote by $\Theta(\mathbf{n}, \mathbf{k}_2, \boldsymbol{\sigma})$, $\hat{\Sigma}(\mathbf{n}, \mathbf{k}_2, \boldsymbol{\sigma})$ and $I_\alpha(\mathbf{n}, \mathbf{k}_2, \boldsymbol{\sigma})$ respectively the estimates of Θ_0 , $\lim_{m \rightarrow \infty} \text{var}(\sqrt{m}(\Theta(\mathbf{n}, \mathbf{k}_2, \boldsymbol{\sigma}) - \Theta_0))$ and the width of the confidence interval $I_\alpha(\Theta(\mathbf{n}, \mathbf{k}_2, \boldsymbol{\sigma}), \hat{\Sigma}(\mathbf{n}, \mathbf{k}_2, \boldsymbol{\sigma}))$. Suppose we have the option of estimating $d(n)$ for one value of $n \in \{1, \dots, N\}$ with known variance $\text{var}(d(n)) = \sigma^2$. We select \tilde{n} as:

$$\tilde{n} = \arg \min_n \mathbb{E}_{d(n) \sim N(k_2(n, \Theta(\mathbf{n}, \mathbf{k}_2, \boldsymbol{\sigma})), \sigma^2)} \left[I_\alpha(\mathbf{n} \cup n, \mathbf{k}_2 \cup \hat{k}_2(n), \boldsymbol{\sigma} \cup \sigma) \right] \quad (8)$$

that is, ‘select the \tilde{n} which will minimise the expected OHS confidence interval width if added to our set \mathbf{n} , with expectation computed with respect to our current parameter estimates’. If no minimum exists, \tilde{n} is selected uniformly from $1, \dots, N$.

Our algorithm is now:

Algorithm 1: Overview of estimation of optimal holdout set size; parametric

Data: A total number n_{add} of times we can afford to estimate $k_2(n)$

- 1 Randomly choose a set \mathbf{n} of $\dim(\Theta)$ values of n in $\{1, \dots, N\}$;
- 2 For all $n \in \mathbf{n}$, make an estimate $\hat{k}_2(n) \in \mathbf{k}_2$ of $k_2(n)$;
- 3 **while** $|\mathbf{n}| < n_{add}$ **do**
- 4 Find best new value \tilde{n} to add to \mathbf{n} as per formula (8);
- 5 Estimate $\hat{k}_2(\tilde{n}) \approx k_2(\tilde{n})$;
- 6 $\mathbf{n} \leftarrow (\mathbf{n} \cup \tilde{n})$, $\mathbf{k}_2 \leftarrow (\mathbf{k}_2 \cup \hat{k}_2(\tilde{n}))$, $\boldsymbol{\sigma} \leftarrow \left(\boldsymbol{\sigma} \cup \sqrt{\text{var}(\hat{k}_2(\tilde{n}))} \right)$
- 7 **end**
- 8 Re-estimate OHS $n_*^{final} = n_*(\Theta(\mathbf{n}, \mathbf{k}_2, \boldsymbol{\sigma}))$;
- 9 **return** n_*^{final}

If we require an asymptotic confidence interval on n_*^{final} , this should be evaluated on a new, independently chosen set of values \mathbf{k}_2 .

The consistency of algorithm 1 generally depends on whether \mathbf{n} eventually contains enough elements of sufficient multiplicity to estimate Θ_0 consistently. If consistency is

of particular concern, sampling some positive proportion of values of \mathbf{n} randomly from $\{1, \dots, N\}$ will guarantee that the multiplicity of all $n \in \mathbf{n}$ eventually exceeds any finite value with probability 1, readily guaranteeing consistency.

The finite-sample bias of n_*^{final} depends on $\nabla_\Theta n_*$ and the variance of Θ . For a power-law form of $k_2(n)$, the value of n_*^{final} is generally biased slightly upwards (see supplementary figure 7 for typical forms of $\nabla_\Theta n_*$).

4.3 Semi-parametric (emulation) estimation of OHS

Parametrisation of $k_2(n)$ may be inappropriate if the learning curve of the risk score or the map \mathcal{L} (from section 4.1) are complex (Viering and Loog, 2021). We propose a second algorithm which is less reliant on assuming a parametric form for $k_2(n)$, using Bayesian optimisation (Brochu et al., 2010). We approximate the cost function ℓ as an *emulator* consisting of a Gaussian process with parametric prior mean function, which allows deviation from parametric assumptions. We take the minimum of its posterior mean over n to be our OHS estimate, efficiently choosing values of n at which to estimate $\ell(n)$ using an ‘expected improvement’ function.

First we must construct an emulator which approximates the cost function. We begin with an initial set of design points \mathbf{n} and their corresponding observed cost estimates \mathbf{d} with sampling variances $\boldsymbol{\sigma}^2$ (noting that $\boldsymbol{\sigma}$ has a slightly different meaning to that in section 4.2). The prior for our emulator is (Vernon et al., 2018):

$$\ell(n) = m(n, \Theta) + u(n) \quad (9)$$

with mean function $m(n, \Theta) = k_1 n + k_2(n; \theta)(N - n)$, given some initial estimate of $\Theta = (N, k_1, \theta)$, and $u(n)$ a zero-mean Gaussian process

$$u(n) \sim \mathcal{GP}(0, k(n, n')) \quad k(n, n') = \sigma_u^2 \exp \left\{ - \left(\frac{n - n'}{\zeta} \right)^2 \right\} \quad (10)$$

where k is chosen to enforce smoothness in $\ell(n)$, though other covariance functions having varying degrees of smoothness could be used (Stein, 1999). The hyperparameters θ , σ_u and ζ are problem-specific and must be specified; however, we will show that for sufficiently large $|\mathbf{n}|$ (with some caveats) mis-specification of θ , σ_u and θ is overcome.

Following McHutchon et al. (2015), we denote

$$d_i \sim N(l(n_i), \sigma_i^2) \quad (11)$$

where $d_i = (\mathbf{d})_i$ is the i th element of \mathbf{d} , etc. Since \mathbf{n} may be a multiset, we take \mathbf{n}^1 as the set of unique values in \mathbf{n} , with \mathbf{d}^1 , $\boldsymbol{\sigma}^1$ defined correspondingly with d_i^1 as an inverse-variance weighted mean of $\{d_j : n_j = n_i^1\}$ with sample variance $(\sigma_i^1)^2$:

$$d_i^1 = \frac{\sum_{j:n_j=n_i^1} \frac{1}{\sigma_j^2} d_j}{\sum_{j:n_j=n_i^1} \frac{1}{\sigma_j^2}} \quad \sigma_i^1 = \left(\sum_{j:n_j=n_i^1} \frac{1}{\sigma_j^2} \right)^{-\frac{1}{2}} \quad (12)$$

noting that σ_i^1 may change with i . Alternatively, we may account for the variation in \mathbf{d} through ‘inactive’ variables and opt to use a ‘nugget’ term (Bower et al., 2010); this approach is described in detail in supplementary section S1.

Now with input n , with an unevaluated loss value, our emulator specifies that the joint distribution of $\ell(n)$ and our observed output values \mathbf{d}^1 is:

$$\begin{bmatrix} \ell(n) \\ \mathbf{d}^1 \end{bmatrix} \sim \mathcal{N} \left(\begin{bmatrix} m(n, \Theta) \\ m(\mathbf{n}^1, \Theta) \end{bmatrix}, \begin{bmatrix} k(n, n) & k(n, \mathbf{n}^1) \\ k(\mathbf{n}^1, n) & k(\mathbf{n}^1, \mathbf{n}^1) + \text{diag}((\boldsymbol{\sigma}^1)^2) \end{bmatrix} \right) \quad (13)$$

where $m(\mathbf{n}^1, \Theta)_i^T = m(n_i^1, \Theta)$, $k(n, \mathbf{n}^1)_i = k(\mathbf{n}^1, n)_i^T = k(n, n_i^1)$, $k(\mathbf{n}, \mathbf{n})_{ij} = k(n_i^1, n_j^1)$, $\text{diag}((\boldsymbol{\sigma}^1)^2)_{ij} = (\sigma_i^1)^2 \mathbf{1}_{i=j}$. By obtaining the conditional posterior distribution $\pi_{\mathbf{n}} \triangleq \pi(\ell(n) | n, \mathbf{n}^1, \mathbf{d}^1, \boldsymbol{\sigma}^1)$ and taking the expectation and variance we gain the Bayes linear update equations (Vernon et al., 2018):

$$\begin{aligned} \mu(n) &= \mathbb{E}_{\pi_{\mathbf{n}}}(\ell(n)) \\ &= m(n, \Theta) + k(n, \mathbf{n}^1)[k(\mathbf{n}^1, \mathbf{n}^1) + \text{diag}((\boldsymbol{\sigma}^1)^2)]^{-1}(\mathbf{d}^1 - m(\mathbf{n}^1, \Theta)) \end{aligned} \quad (14)$$

$$\begin{aligned} \Psi(n) &= \text{var}_{\pi_{\mathbf{n}}}(\ell(n)) \\ &= k(n, n) - k(n, \mathbf{n}^1)[k(\mathbf{n}^1, \mathbf{n}^1) + \text{diag}((\boldsymbol{\sigma}^1)^2)]^{-1}k(\mathbf{n}^1, n) \end{aligned} \quad (15)$$

In algorithm 1, selection of new design points should generally favour well-spaced points across $\{1, \dots, N\}$ for both exploration and exploitation purposes. In this case, since we wish both to estimate the OHS accurately but also locally approximate ℓ well, we choose the next n in a way which predominantly (but not completely) favours exploitation. We use the ‘expected improvement’, which measures discrepancy between the emulator at a certain design point and the known minimum $EI(\cdot)$ (Brochu et al., 2010):

$$EI(n) = (d^- - \mu(n))\Phi\left(\frac{d^- - \mu(n)}{\sqrt{\Psi(n)}}\right) + \sqrt{\Psi(n)}\phi\left(\frac{d^- - \mu(n)}{\sqrt{\Psi(n)}}\right) \quad (16)$$

where $d^- = \min_i\{\mathbf{d}^1_i\}$, and

$$\tilde{n} = \arg \max_{n \in \{1, \dots, N\}} EI(n) \quad (17)$$

$$\begin{aligned} &= \arg \max \left\{ \int_{-\infty}^{d^-} d^- d\pi_{\mathbf{n}} - \int_{-\infty}^{d^-} \ell(n) d\pi_{\mathbf{n}} \right\} \\ &= \arg \max \left\{ \int_{-\infty}^{d^-} (d^- - \ell(n)) d\pi_{\mathbf{n}} \right\} \\ &= \arg \max \left\{ \int_{\mathbb{R}} \max\{0, d^- - \ell(n)\} d\pi_{\mathbf{n}} \right\} \\ &= \arg \max \left\{ \mathbb{E}_{\pi_{\mathbf{n}}}(\max\{0, d^- - \ell(n)\}) \right\} \end{aligned} \quad (18)$$

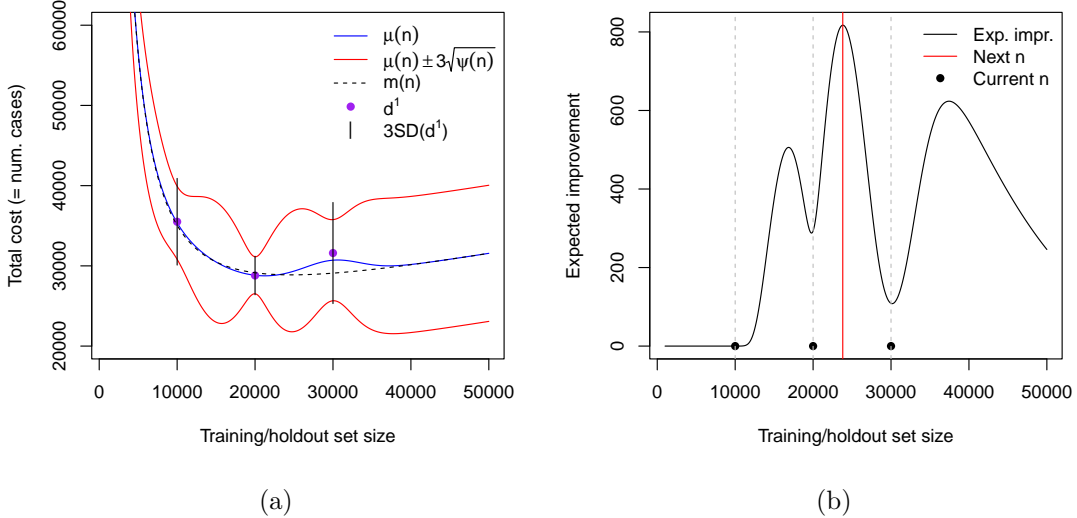


Figure 2: Left panel shows emulator constructed using three $k_2()$ values (see pipelines). Function $m(n, \Theta)$ is constructed using θ derived from these three $k_2()$ estimates. Note reduced pointwise posterior variance at sample points. Rightmost panel shows expected improvement plot for the emulator constructed in figure 2a. Note local minima at existing sample points.

By formulating the problem in terms of $EI(\cdot)$, there is a natural stopping criterion on the size of \mathbf{n} : setting a threshold $EI(\hat{n}) > \tau$ allows us to specify that for each iteration that we expect total cost to improve by at least τ over our current known minimum d^- . This leads to the following algorithm for OHS estimation by Bayesian Emulation:

Algorithm 2: Overview of estimation of optimal holdout set size; emulation

Data: A value τ specifying minimum improvement in total cost

- 1 Choose initial values \mathbf{n} randomly from $\{1, \dots, N\}$ with $|\mathbf{n}| > \dim(\Theta)$;
- 2 Estimate costs $d_i = d(n_i) \approx \ell(n_i)$ with errors $\sigma_i = \sqrt{\text{var}(d(n_i))}$;
- 3 Coalesce $\mathbf{n}, \mathbf{d}, \boldsymbol{\sigma}$ into $\mathbf{n}^1, \mathbf{d}^1, \boldsymbol{\sigma}^1$ as above;
- 4 Estimate functions $\mu(n), \Psi(n), EI(n)$, with $\Theta = \Theta(\mathbf{n}^1, \mathbf{d}^1, \boldsymbol{\sigma}^1)$;
- 5 **while** $\max_{n \in \{1, \dots, N\}} \{EI(n)\} > \tau$ **do**
- 6 $\tilde{n} \leftarrow \arg \max_{n \in \{1, \dots, N\}} EI(n)$;
- 7 Estimate $d(\tilde{n}) \approx k_2(\tilde{n})$;
- 8 $\mathbf{n} \leftarrow (\mathbf{n} \cup \tilde{n}); \mathbf{d} \leftarrow (\mathbf{d} \cup d(\tilde{n})); \boldsymbol{\sigma} \leftarrow \left(\boldsymbol{\sigma} \cup \sqrt{\text{var}(d(\tilde{n}))} \right)$;
- 9 Coalesce $\mathbf{n}, \mathbf{d}, \boldsymbol{\sigma}$ into $\mathbf{n}^1, \mathbf{d}^1, \boldsymbol{\sigma}^1$;
- 10 Re-estimate functions $\mu(n), \Psi(n), EI(n)$, with $\Theta = \Theta(\mathbf{n}^1, \mathbf{d}^1, \boldsymbol{\sigma}^1)$;
- 11 **end**
- 12 **return** $n_*^{final} = \arg \min_{n \in \{1, \dots, N\}} \{\mu(n)\}$

Various results on the consistency of the expected improvement algorithm have been proved, albeit in differing settings; either with noiseless observations \mathbf{d} (Locatelli, 1997; Vazquez and Bect, 2010; Bull, 2011) or with noisy observations with known variance (Ryzhov, 2016). We prove the following consistency results specifically for the setting of this work in Appendix A3.

Theorem 3. *If $\ell(n), \boldsymbol{\sigma}$, and $m(n, \Theta)$ are almost surely bounded and $d_i \sim N(l(n_i), \sigma_i^2)$ then for every $n \in \{1, \dots, N\}$, as the multiplicity of n in \mathbf{n} tends to ∞ we have $\mu(n) \rightarrow \ell(n)$ and $\Psi(n) \rightarrow 0$ almost surely with respect to variation in \mathbf{d} .*

This result asserts that $\mu(n)$ can eventually approximate any loss function sufficiently well given enough estimates of ℓ at all values of n . It is not obvious that this is guaranteed by algorithm 2, although we show that this generally does occur in the following, the proof of which is given in Appendix A3:

Theorem 4. *If $\ell(n), \boldsymbol{\sigma}$, and $m(n, \Theta)$ are almost surely bounded and $d_i \sim N(l(n_i), \sigma_i^2)$ then under algorithm 2 with $\tau = 0$, the value $\mu(\tilde{n})$ converges almost surely to $\ell(\tilde{n})$ for every $\tilde{n} \in \{1, \dots, N\}$.*

We characterise the error in n_* using ‘the number of values of n for which the probability of the true cost at holdout set size n is less than the estimated minimum cost exceeds $1 - \alpha$ ’, or formally:

$$S_\alpha = \{n : P_{\mathbf{n}_\pi}(\ell(n) < \mu(n_*)) \geq 1 - \alpha\} \quad (19)$$

although this should not be interpreted as a credible set for n_* . This is implemented in our R package `OptHoldoutSize`, available on CRAN.

5 Simulations

5.1 Example

In this section, we analyse the dynamics of a roughly realistic, binary outcome system, subject to predictions from different families of risk models. Our main aim is to demonstrate the natural emergence of an OHS from a reasonable setting.

We generated datasets with a population size $N = 5000$ with seven standard normally distributed covariates and outcomes Y under a ground-truth logistic model, either with interaction terms (i.e., non-linear) or without (linear). We considered risk scores ρ derived from either logistic regression models (not including interaction terms) or random forests. We designated random-valued cost functions C_1, C_2 , as

$$C_i(X_j) = \begin{cases} 0 & \text{if } \hat{Y}_j = 0 \text{ and } Y_j = 0 & (TN) \\ 0.5 & \text{if } \hat{Y}_j = 1 \text{ and } Y_j = 0 & (FP) \\ 0.5 & \text{if } \hat{Y}_j = 1 \text{ and } Y_j = 1 & (TP) \\ 1 & \text{if } \hat{Y}_j = 0 \text{ and } Y_j = 1 & (FN) \end{cases} \quad (20)$$

where $\hat{Y}_j \in \{0, 1\}$ is sample j 's class as predicted by the risk model given X_j , and Y_j is the observed incidence of Y .

Figure 3 shows the results of the simulation under this setup, using either linear or logistic prediction models and linear or non-linear underlying models for $Y|X$. We can observe that an OHS can arise naturally from standard predictive models, since empirical k_2 curves for both a random forest and logistic regression satisfy assumptions 2 and 4. The OHS occurs at a value n smaller than that at which $k_2(n)$ is nearly ‘flat’, indicating that unnecessarily large training sets are suboptimal. However, since $\ell(n)$ rises only linearly as n increases, it is generally less costly to slightly overestimate rather than underestimate the OHS. Finally, the rightmost panels illustrate that the OHS is not necessarily smaller for a more accurate model: the random forest model (non-lin ρ) in the non-linear underlying case (right panels) leads to uniformly lower expected costs $k_2(n)$ at all potential holdout set sizes, although the *optimal* holdout set size is larger.

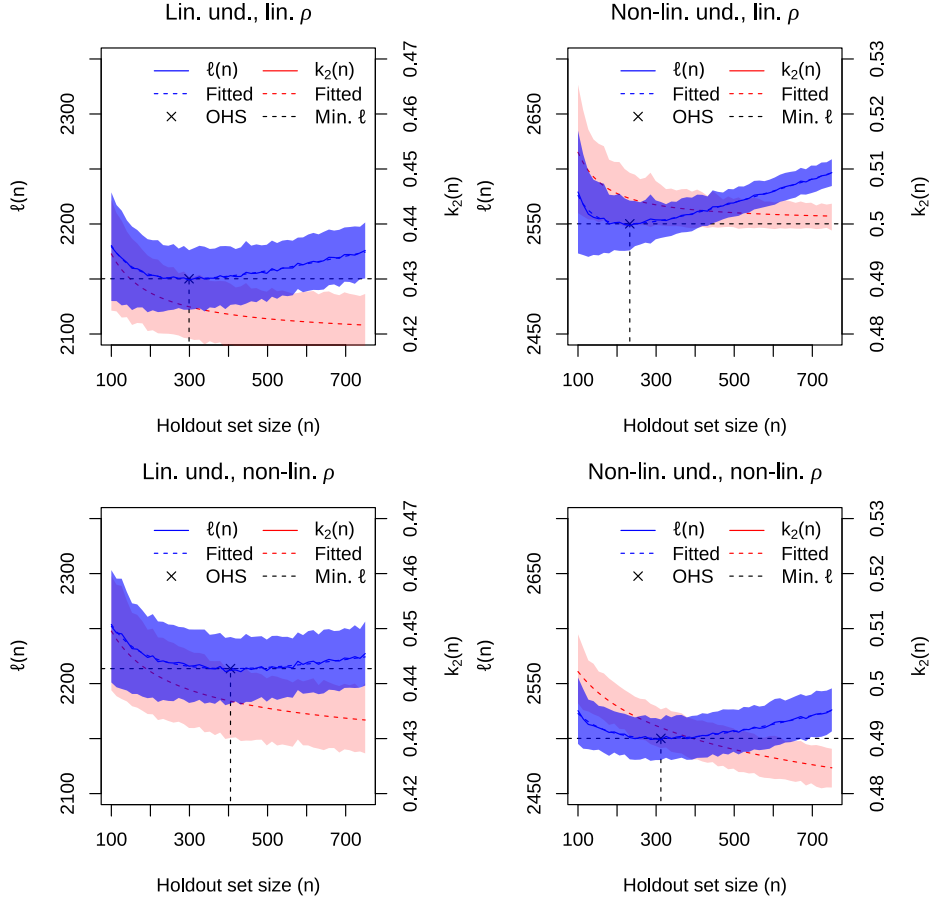


Figure 3: Examples of cost functions as per Theorem 1 arising naturally from a basic risk score, with varying underlying model (und.), risk score type (ρ) and one point-wise standard deviation (shaded regions). The contributions of terms $k_1 n$ to $\ell(n)$ depend only on the underlying model and are the same in each column.

5.2 Comparison of parametric and emulation algorithms

In this section, we demonstrate circumstances in which either one of the proposed algorithms may be preferable to the other. We consider two versions of the function $k_2(n)$

$$k_2^p(n) = an^{-b} + c \quad \text{and} \quad k_2^{np}(n) = an^{-b} + c + 10^4 \phi \left(\frac{n - 4 \times 10^4}{8 \times 10^3} \right)$$

where ‘p’/‘np’ denotes ‘parametric assumptions satisfied/not satisfied’, and $\theta = (a, b, c) = (10000, 1.2, 0.2)$. The function $k_2^{np}(n)$ exhibits ‘double-descent’ behaviour (figure 4a), which

is possible for various learning curves (Viering and Loog, 2021). Corresponding cost functions are shown in figure 4b. We assume N and k_1 are known to be 1×10^5 and 0.4 respectively. For emulation, we use a kernel width $\zeta = 5000$ and variance σ_u^2 of 1×10^7 .

The double-descent form of k_2 does not satisfy the assumptions of Theorem 1, but in our case leads to a single single optimal holdout set size nonetheless. We note that more subtle misparametrisations will also lead to inconsistency in OHS estimation if the parametric approach is used; for instance, if $k_2(n)$ follows exponential decay but is parametrised using a power-law curve.

We firstly show the distribution of estimates of OHS using our two algorithms when k_2 takes either form above. To fit k_2 , we use \mathbf{n} given by 200 values of n randomly chosen from $\{1, \dots, N\}$, with values \mathbf{k}_2 independently sampled as $(\mathbf{k}_2)_i \sim N(k_2(n_i), \sigma_i^2)$, where $\sigma \sim U(0.001, 0.02)$. Figure 4c shows the distributions and medians of OHS estimates using the parametric and emulation algorithm in settings with parametric assumptions either satisfied or unsatisfied.

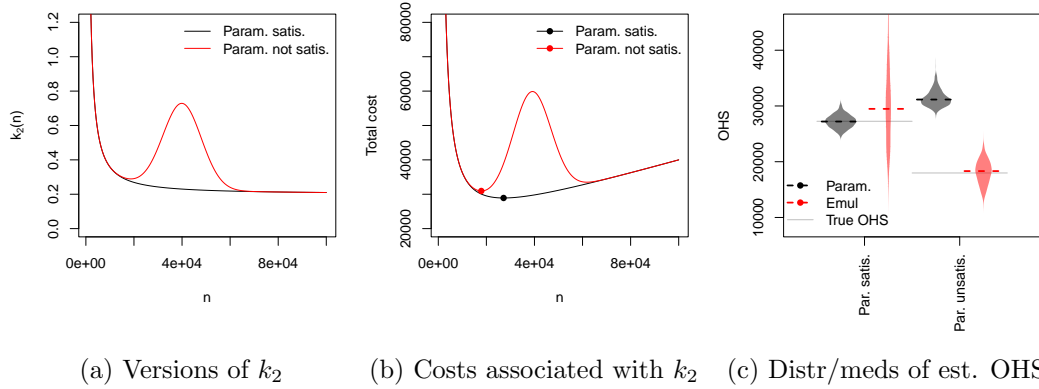


Figure 4: Parametric and emulation algorithms with parametric assumptions satisfied or unsatisfied

The parametric OHS estimate is empirically unbiased and has less variance than the emulation estimate when parametric assumptions are satisfied, but is biased when they are not. The variance of OHS estimates using the emulation method is lower when parametric assumptions are not satisfied because the true cost function has a sharper minimum in that case (see figure 4b). Because the cost function is ‘flat’ around the minimum in the setting where parametric assumptions are satisfied (figure 4b), the consequences of the high variance of the semi-parametric (emulation) estimator are minimal, as the cost is similar across a range of values near the OHS.

We next examine the consequences of sampling \tilde{n} (the ‘next’ value of n) greedily (using equation (8) as in algorithm 1 or EI as in algorithm 2), rather than randomly (\tilde{n} chosen uniformly in $\{1, \dots, N\}$), by comparing the rates of convergence of OHS estimates. Figure 5 show medians and (roughly) a discrete kernel estimate of optimal holdout size estimates at

various sizes of $|\mathbf{n}|$, where \mathbf{n} is generated by adding points \tilde{n} either randomly systematically (after choosing the initial five values in \mathbf{n} randomly). Convergence is faster when ‘next points’ are picked systematically rather than randomly. Convergence is also faster when using parametric estimates, though again parametric estimates are biased and inconsistent when parametric assumptions are not satisfied. This is highlighted by the smaller panels which show the root mean-square error between the total cost at the estimated optimal sizes and the total cost at the true OHS: as expected the parametric algorithm is to be favoured where the assumptions are satisfied and the non-parametric where they are not. Note in particular, that the non-parametric method shows bifurcation detecting both local minima whilst the parametric method converges to a mid-point which is far from optimal in terms of total costs.

5.3 Illustration in realistic setting

In this section, we describe a potential practical end-to-end implementation of our algorithm in a healthcare setting. We describe possible motivations for updating and harms of updating naïvely, a practical set-up of a hold-out set procedure, estimation of requisite parameters of the function $\ell(\cdot)$, and computation of an optimal holdout set size and associated error. We consider the ASPRE score (Akolekar et al., 2013) for evaluating risk of pre-eclampsia (PRE), a hypertensive complication of pregnancy, on the basis of predictors derived from ultrasound scans in early pregnancy. Although treatable, PRE confers a serious risk to both the fetus and the mother. The risk of pre-eclampsia is lowered by treatment with aspirin through the second and third trimesters (Rolnik et al., 2017b), but aspirin therapy itself confers a slight risk, contraindicating universal treatment, and suggesting prescription of aspirin only if the risk of PRE is sufficiently high or other indications are present (LeFevre, 2014; ACOG, 2016). The ASPRE score was developed to aid clinicians in estimating PRE risk (Wright et al., 2012) and has been shown to be useful in prioritising patients for aspirin therapy (Rolnik et al., 2017a). We will not differentiate early- and late-stage PRE.

It may be desirable to update the ASPRE score in future for several reasons. Firstly, inclusion of additional covariates or more sophisticated machine-learning methods may be of benefit (Akolekar et al., 2013), and distributions of covariate values across the population may change with population demographic shift over time (e.g. maternal serum placental growth factor, (Yang et al., 2016)), necessitating changes to the ways that such covariates are used in the model. However, as discussed in Section 1, a difficulty in updating models in this way arises from the possible effect of the ASPRE score itself: namely, a naïve re-fitting of a risk score on the basis of $(X :)$ maternal assessment in early pregnancy and $(Y :)$ eventual PRE incidence could lead to dangerous underestimation of PRE risk, due to individuals previously assessed as high risk being treated in response to the assessment.

Retraining a new model on a held-out set could avoid this problem. For such a hold-out set, no ASPRE score would be calculated at the first ultrasound scan, and patients would

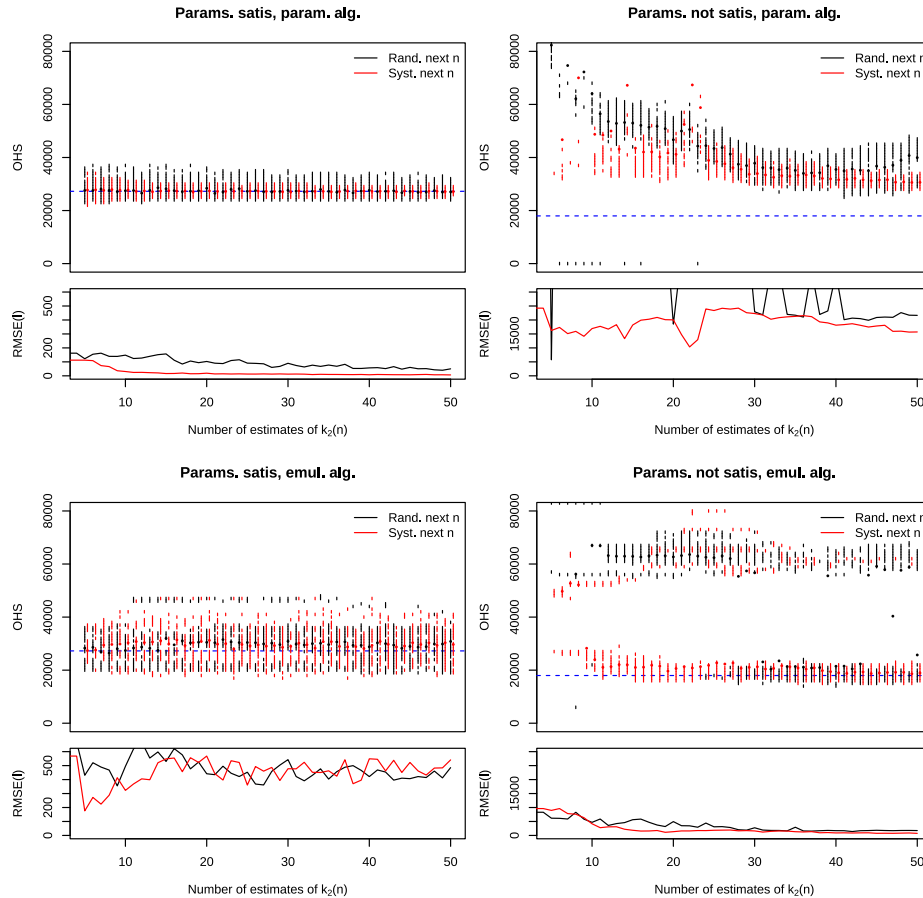


Figure 5: Comparison of convergence rates with parametric and emulation algorithms, using either a random or greedy method to select the next value of n to add to \mathbf{n} . All algorithms are run for 200 datasets simulated from the underlying model. In the larger panels, dashed horizontal lines show the true OHS, while vertical lines indicate when at least 2.5% of runs of the algorithm select the next value of n within a grid of size 1000 (ie a form of discrete kernel estimate). Smaller panels show the root mean-square error between the total costs at each of the 200 proposed n and the minimal total costs at the true OHS. Note variable axis scaling on left and right.

be treated according to best practice in the absence of a risk score. An updated score would then be fitted to data from such patients. An obvious concern is that patients in this holdout set go without the benefit of the ASPRE score, leading to a less accurate allocation of prophylactic treatment (aspirin) and consequently a higher risk of PRE (Rolnik et al., 2017a), which may indicate using the smallest possible holdout set. However, an inappropriately small hold-out set would lead to an inaccurate updated model, reducing the benefit of future use of the score. This vividly illustrates the tension at the heart of model updating which we seek to address in this work.

If we suppose that ASPRE is to be refitted every five years, then the ‘intervention set’ should include all individuals in the subsequent years before the model is refitted, and all individuals not used in the next refitting procedure. Suppose we are refitting ASPRE to use in a population of 5 million individuals, from which we have approximately 80,000 new pregnancies per year. Thus $N \approx 400,000$ (SE: 1500). See supplementary section S2 for further details.

We presume a simple clinical action in which a fixed proportion $\pi = 10\%$ of individuals at the highest assessed PRE risk are treated with aspirin. We assume that if untreated with aspirin, a proportion π_0 of individuals designated to be ‘low-risk’ (lowest 90%) will develop PRE, as will a proportion π_1 of individuals designated high-risk. Under current pre-ASPRE best-practice guidelines O’Gorman et al. (2017) we have $\pi_0 \approx 0.02$ (SE 0.0009) and $\pi_1 \approx 0.08$ (SE 0.008) (see supplementary section S2). Aspirin reduces PRE risk by approximately $1 - \alpha = 63\%$ (SE 0.09) (Rolnik et al., 2017b). We denote ‘cost’ as simply the number of cases of PRE in a population, so we expect a total expected cost per individual under ‘baseline’ treatment (ie clinical actions without the aid of a risk model) proportional to

$$k_1 = \pi_0(1 - \pi) + \pi_1\pi\alpha \approx 0.022 \quad (21)$$

with standard error approximately 0.001. Note that this is not equal to the untreated PRE risk in the population, since some proportion of individuals are treated pre-emptively.

The data used to fit the initial ASPRE model can be used to estimate the learning curve for potential model updates: at the stage at which the ASPRE score was first fitted, the optimal ‘holdout set’ size is as large as possible. We do not have access to this dataset, but demonstrate estimation of a learning curve on ‘mockup’ data designed to resemble it. Although $k_2(n)$ is easy and fast to estimate here, in order to mimic a real example where such estimation is time consuming or costly we restrict ourselves to use only $|\mathbf{n}| = 120$ values of n , determined using either algorithm 1 or 2. For both algorithms, we assumed a power-law form $k_2(n; \theta = (a, b, c)) = an^{-b} + c$.

Using the parametric algorithm, we found an OHS of 10271 (90% CI 8103-12438), with minimum cost (expected number of cases over five years) of 8172. Using the emulation algorithm, we found an OHS of 13313 with an expected cost of 8164, with holdout sizes of 9210-17619 having a probability > 0.1 of an expected cost < 8164 . Figure 6 shows estimated cost functions, optimal holdout sizes, and error using the two algorithms.

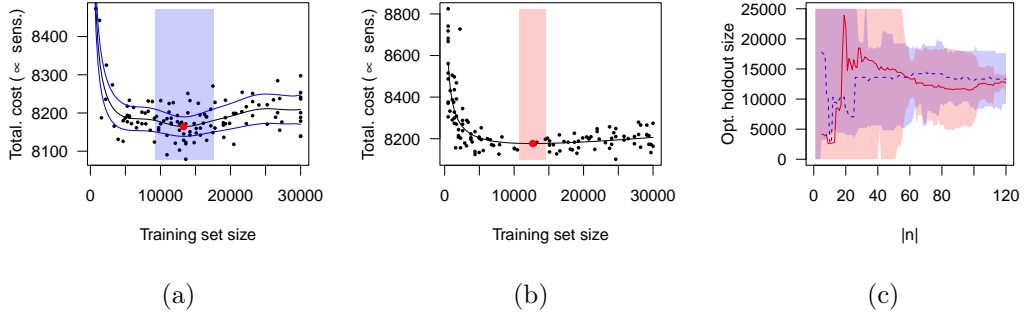


Figure 6: Estimation of cost functions, OHS and error using parametric (right) and emulation (middle) algorithms, and track of estimated OHS with number of sample points $|n|$ on right. Note that the ‘best’ points to optimise parametric estimation tend to be spread-out, to estimate θ well, but for the emulation method they tend to be close to the OHS to locally approximate the cost function well. Error measures in parametric and emulation algorithms have different meanings and are not comparable.

6 Discussion

In this work we establish theoretically the existence of an optimal holdout set size under reasonable assumptions, establish two algorithms for estimating this optimal holdout size, and evaluate their use in both a toy simulation and a real-life motivated simulation. We establish a practical and simple approach to an important contemporary problem in modern machine learning, which will become particularly important as risk scores become more widely used in real-world applications.

Theorem 1 establishes that straightforward conditions on the system to be modelled lead to an OHS which is straightforward to find, and indeed that the cost function is convex (in a discrete sense). An obvious limitation is the requirement for convexity of k_2 ; risk score learning curves, on which k_2 depends, are not necessarily convex for complex models (Viering and Loog, 2021). In practice, the cost function $\ell(n)$ is still generally well-behaved even if convexity of k_2 is violated, and may be approximated using our emulation algorithm (as demonstrated in figures 4b, 5).

The use of a Gaussian process emulator to approximate the true loss function enables an automatic selection of the optimal holdout set size under fewer assumptions, although the efficiency of this method heavily depends on the quality of our emulator. Various extensions of the emulator may improve our surrogate of the loss function, for example specifying priors on the parameters $\theta, \sigma_u^2, \zeta$ and using the likelihood provided by the Gaussian process to marginalise out these parameters. An explicit approach is given in Andrianakis and Challenor (2011), but under linearity assumptions which do not hold in our case, so analytic

tractability would be lost. If we were able to cheaply estimate the derivative of the cost function at design points, this could be incorporated into our emulator (Killeya, 2004), enabling greater posterior accuracy around these points. Direct estimation of gradients from only estimates of $\ell(n)$ usually requires double the number of evaluations as estimation of $\ell(n)$ values, and so has the potential to become a more costly procedure than the method presented in section 4.3.

We have generally assumed that the function k_2 is to be estimated by repeated noisy observation of pairs $(n, k_2(n))$. It is possible that k_2 could be estimated in other ways or be known *a priori*. Testing the impact of a risk score is generally a difficult problem (Ben-Israel et al., 2020) and is unavoidable in OHS estimation, although is also necessary to justify deployment. If a risk score can not in any way affect interventions (for instance, a risk score for surgical complications (Nashef et al., 2012) used exclusively to discuss risk with patients) then $k_2(n)$ is constant and no holdout set scheme is needed for updating. We emphasise that even indirect action on risk scores (for instance, using a medical risk score to identify at-risk demographic classes for budgetary planning) lead to risk scores being ‘victims of their own success’ (Lenert et al., 2019) and require planning of an updating strategy.

Other solutions to the model updating problem have been proposed, such as developing models that introduce missing causal connections Alaa and van der Schaar (2018); Sperrin et al. (2019) and using several predictive scores together Liley (2021). Such solutions tend to be difficult to implement: more comprehensive modelling generally requires some observation of the intervention, requiring further samples or more data across time, and parallel use of several risk scores is difficult to implement. With this in mind, holdout sets could prove valuable in updating strategies since, in principle, they can be applied in any setting. Moreover, as suggested by Sperrin et al. (2019), forced availability of direct data for the underlying distribution of (X, Y) through the holdout set in itself facilitates post-deployment maintenance and surveillance.

In summary, we demonstrate that standard settings for predictive risk scores give rise to optimal holdout set sizes, and develop tractable approaches to finding them. In particular, we strongly suggest planning an updating strategy for a risk model *before* it is deployed. This work illustrates one strategy in this direction and we hope stimulates both use of and extensions of such methods for safe predictive score updating.

Acknowledgements

SH's contributions arose from an MSc dissertation undertaken on the MISCADA programme at Durham University.

JL and LJMA were partially supported by Wave 1 of The UKRI Strategic Priorities Fund under the EPSRC Grant EP/T001569/1, particularly the "Health" theme within that grant and The Alan Turing Institute; and were partially supported by Health Data Research UK, an initiative funded by UK Research and Innovation, Department of Health and Social Care (England), the devolved administrations, and leading medical research charities; SRE is funded by the EPSRC doctoral training partnership (DTP) at Durham University, grant reference EP/R513039/1; LJMA was partially supported by a Health Programme Fellowship at The Alan Turing Institute.

JL is grateful to the Research Design Service North-East for part-funding their position.

We acknowledge the SPARRA project (Public Health Scotland/Alan Turing institute) as an example of a risk score used on a population-wide scale, which had a large role in incentivising this project.

We thank Dr Catalina Vallejos (University of Edinburgh), Professor Sebastian Vollmer (German Research Centre for Artificial Intelligence) and Dr Bilal Mateen (Kings College London Hospital, Wellcome Trust) for helpful discussion.

Code availability

We have implemented all functionality described in this manuscript in an R package on CRAN (`OptHoldoutSize`) and at <https://github.com/jamesliley/OptHoldoutSize>. Pipelines to generate all results in this manuscript are available at https://github.com/jamesliley/OptHoldoutSize_pipelines.

A1 Proof of Theorem 1

Theorem 1. *Suppose assumptions 1-4 hold. Then there exists a $N_* \in (0, N)$ with $N \in \mathbb{N}$, which we call the optimal holdout set size, such that:*

$$\begin{aligned}\ell(i) &\geq \ell(j) \text{ for } 0 < i < j < N_* \\ \ell(i) &\leq \ell(j) \text{ for } N_* < i < j < N\end{aligned}$$

Proof. As above, we may impose that

$$\frac{\partial}{\partial n} k_2(n) < 0 \quad (22)$$

Since both $k_2(n)$ and $(N - n)$ are positive and monotonically decreasing in n , so is $k_2(n)(N - n)$. Now

$$\ell'(n) = \frac{\partial}{\partial n} (k_1 n + k_2(n)(N - n)) \quad (23)$$

$$= k_1 + k_2'(n)(N - n) - k_2(n) \quad (24)$$

$$= (k_1 - k_2(n)) + k_2'(n)(N - n) \quad (25)$$

By assumption 3, $k_1 < k_2(0)$, and, from equation (22), $k_2'(0) < 0$, so both terms in equation (25) are negative when $n = 0$ and $\ell'(0) < 0$. When $n = N$, the second term vanishes while the first one is positive, as $k_1 > k_2(N)$ by assumption 3. We thus have $\ell'(N) > 0$. By assumption, ℓ is smooth, so by Bolzano's Theorem, there must exist at least one point n_* for which $\ell'(n_*) = 0$, which is an extremum of ℓ .

We now prove that this extremum is unique and a minimum. First, by assumption 4, we may impose that

$$\frac{\partial^2}{\partial n^2} k_2(n) > 0 \quad (26)$$

Taking the second derivative of ℓ

$$\frac{\partial^2}{\partial n^2} \ell(n) = \frac{\partial^2}{\partial n^2} (k_1 n + k_2(n)(N - n)) \quad (27)$$

$$= k_2''(n)(N - n) - 2k_2'(n) \quad (28)$$

and using equations (22) and (26), we see that $\ell''(n)$ is strictly positive, and, as a consequence, $\ell'(n)$ is monotonically increasing. Therefore, the extremum of $\ell(n)$ at n_* we found earlier is unique and, as $\ell''(n) > 0$, it is a minimum.

If $n_* \in 1..(N - 1)$, let $N_* = n_*$. If $n_* \notin \mathbb{N}$, let N_* be the closest natural number to either side of n_* . From assumption 3, N_* cannot be 0 or N . In both scenarios, this completes the proof. \square

A2 Analysis of robustness

As above, we consider n_* as a function of parameters $\Theta = (N, k_1, \theta)$ (where $k_2(\cdot) = k_2(\cdot; \theta)$), write $n_* = n_*(\Theta)$, set $\Theta_0 = \mathbb{E}(\Theta)$, $n_0 = n_*(\Theta_0)$ and $\ell(n_0) = \ell(n_0; \Theta_0)$ and $\ell(n_*) = \ell(n_*(\Theta), \Theta)$. As discussed above, n_* and $\ell(n_*)$ do not generally have means or standard errors.

Theorem 2. *Assume that $k_2''(n; \theta)$, $k_2'(n; \theta)$ and $\nabla_\theta k_2(n; \theta)$ are continuous in n and θ in some neighbourhood of (n_0, Θ_0) , and that Θ_0 parametrises a setting satisfying assumptions 1-4. Suppose that Θ behaves as a mean of m appropriately-distributed samples in satisfying $\sqrt{m}(\Theta - \Theta_0) \rightarrow_d N(0, \Sigma)$ where Θ_0 does not depend on m , that an estimate $\hat{\Sigma}$ of Σ is available which is independent of Θ and satisfies $\|\hat{\Sigma} - \Sigma\|_2 \rightarrow_d 0$, and that n_0 is finite and unique as above. Then denoting*

$$\beta_\Theta = \frac{\frac{\partial^2 \ell}{\partial n \partial \Theta_i}}{\frac{\partial^2 \ell}{\partial n^2}}, \quad \gamma_\Theta = \frac{\partial \ell}{\partial \Theta_i}$$

we may uniquely define $n_0 = \{n : \ell'(n; \Theta_0) = 0\}$ and we have

$$\sqrt{m}(n_* - n_0) \rightarrow_d N(0, \beta_{\Theta_0}^t \Sigma \beta_{\Theta_0}), \quad \sqrt{m}(\ell(n_*) - \ell(n_0)) \rightarrow_d N(0, \gamma_{\Theta_0}^t \Sigma \gamma_{\Theta_0}) \quad (29)$$

and the confidence intervals

$$I_\alpha(\Theta, \hat{\Sigma}) = \left[n_*(\Theta) - z_\alpha \sqrt{\frac{\beta_{\Theta_0}^t \hat{\Sigma} \beta_{\Theta_0}}{m}}, n_*(\Theta) + z_\alpha \sqrt{\frac{\beta_{\Theta_0}^t \hat{\Sigma} \beta_{\Theta_0}}{m}} \right]$$

$$J_\alpha(\Theta, \hat{\Sigma}) = \left[\ell(n_*) - z_\alpha \sqrt{\frac{\gamma_{\Theta_0}^t \hat{\Sigma} \gamma_{\Theta_0}}{m}}, \ell(n_*) + z_\alpha \sqrt{\frac{\gamma_{\Theta_0}^t \hat{\Sigma} \gamma_{\Theta_0}}{m}} \right]$$

where $z_\alpha = \Phi^{-1}(1 - \frac{\alpha}{2})$, satisfy $P(n_0 \in I_\alpha(\Theta, \hat{\Sigma})) \rightarrow 1 - \alpha$ and $P(\ell(n_0) \in J_\alpha(\Theta, \hat{\Sigma})) \rightarrow 1 - \alpha$ as $m \rightarrow \infty$.

Proof. From $\ell(n) = k_1 n + k_2(n; \theta)(N - n)$ and $n_* = \{n : \ell'(n; \Theta) = 0\}$, where such n_* is unique, we have (as per section 4.2)

$$(\nabla n_*)_i = \frac{\partial n_*}{\partial \Theta_i} = \frac{\frac{\partial^2 \ell}{\partial n \partial \Theta_i}}{\frac{\partial^2 \ell}{\partial n^2}} = (\beta_{\Theta_0})_i$$

$$(\nabla \ell(n_*))_i = \frac{\partial \ell}{\partial \Theta_i} = (\gamma_{\Theta_0})_i$$

for all components Θ_i of Θ . Thus partial derivatives of n_* exist as long as

$$\frac{\partial^2 \ell}{\partial n^2} > 0 \quad (30)$$

By assumption, $\ell(\cdot; \Theta_0)$ has a minimum at n_0 . Since

$$\frac{\partial^2 \ell}{\partial n^2} = \frac{\partial^2}{\partial n^2} k_2(n; \theta) - 2 \frac{\partial}{\partial n} k_2(n; \theta) \quad (31)$$

where both terms are continuous in a neighbourhood of n_0 , Θ_0 by assumption, the value of $\frac{\partial^2 \ell}{\partial n^2}$ must be positive in some (possibly smaller) neighbourhood R_δ of (n_0, Θ_0) of width 2δ , and hence all partial derivatives of n_* and $\ell(n_*)$ are defined (and indeed continuous) in R_δ . Within R_δ we have

$$\begin{aligned} n_*(\Theta) &= n_*(\Theta_0) + (\nabla n_*|_{\Theta=\Theta_0}) \cdot (\Theta - \Theta_0) + O(\|\Theta - \Theta_0\|_2) \\ &= n_0 + \beta_{\Theta_0}^t \cdot (\Theta - \Theta_0) + O(\|\Theta - \Theta_0\|_2) \end{aligned} \quad (32)$$

$$\begin{aligned} \ell(n_*) &= \ell(n_*(\Theta_0); \Theta_0) + (\nabla \ell(n_*)|_{\Theta=\Theta_0}) \cdot (\Theta - \Theta_0) + O(\|\Theta - \Theta_0\|_2) \\ &= \ell(n_0) + \gamma_{\Theta_0}^t \cdot (\Theta - \Theta_0) + O(\|\Theta - \Theta_0\|_2) \end{aligned} \quad (33)$$

from which, given the assumption of asymptotic normality of Θ , assertions (29) follow. We note that despite this convergence in distribution, n_* and $\ell(n_*)$ do not generally have first or second moments for finite m .

We now have

$$\begin{aligned} P\left(n_0 \geq n_*(\Theta) + z_\alpha \sqrt{\frac{\beta_\Theta \widehat{\Sigma} \beta_\Theta^t}{m}}\right) &= P\left(\frac{\sqrt{m}}{z_\alpha} (n_0 - n_*(\Theta)) \geq \sqrt{\beta_\Theta^t \widehat{\Sigma} \beta_\Theta}\right) \\ &= P\left(\frac{\sqrt{m}}{z_\alpha} (n_0 - n_*(\Theta)) \geq (\beta_{\Theta_0}^t \Sigma \beta_{\Theta_0} + \beta_\Theta^t (\widehat{\Sigma} - \Sigma) \beta_\Theta + (\beta_\Theta - \beta_{\Theta_0})^t \Sigma (\beta_\Theta + \beta_{\Theta_0}))^{\frac{1}{2}}\right) \\ &\rightarrow P\left(\frac{\sqrt{m}}{z_\alpha} (n_0 - n_*(\Theta)) \geq \sqrt{\beta_{\Theta_0}^t \Sigma \beta_{\Theta_0}}\right) \\ &= \frac{\alpha}{2} \end{aligned} \quad (34)$$

since, by the assumption of convergence of $\widehat{\Sigma}$

$$\begin{aligned} \left| \beta_\Theta^t (\Sigma - \widehat{\Sigma}) \beta_\Theta \right| &\leq \|\beta_\Theta\|_2 \|\Sigma - \widehat{\Sigma}\|_2 \\ &\rightarrow_p 0 \end{aligned} \quad (35)$$

and, since $P(\Theta \in R_\delta) \rightarrow 1$ by the asymptotic normality of Θ , we have from (32)

$$|(\beta_\Theta - \beta_{\Theta_0})^t \Sigma (\beta_\Theta + \beta_{\Theta_0})| = O(\|\beta_\Theta - \beta_{\Theta_0}\|_2)$$

$$\rightarrow_p 0 \quad (36)$$

Thus, combining with the corresponding limit for the lower end of $I_\alpha(\Theta, \hat{\Sigma})$:

$$P(n_0 \in I_\alpha(\Theta, \hat{\Sigma})) \rightarrow 1 - \alpha \quad (37)$$

as required. An identical argument holds for $J_\alpha(\Theta, \hat{\Sigma})$. \square

If we assume a power-law form of k_2 , parametrised by $\theta = (a, b, c, k_1, N)$;

$$k_2(n; \theta) = an^{-b} + c \quad (38)$$

then we have

$$\begin{aligned} \frac{\partial n_*}{\partial a} &= \frac{1}{a} \left(\frac{bNn_* - (b-1)n_*^2}{b(b+1)N - b(b-1)n_*} \right) \\ \frac{\partial n_*}{\partial b} &= \frac{Nn_*(b \log(n_*) - 1) - n_*^2((b-1) \log(n_*) - 1)}{b(b+1)N - b(b-1)n_*} \\ \frac{\partial n_*}{\partial c} &= \frac{1}{a} \left(\frac{n_*^{b+2}}{b(b+1)N - b(b-1)n_*} \right) \\ \frac{\partial n_*}{\partial k_1} &= \frac{1}{a} \left(\frac{-n_*^{b+2}}{b(b+1)N - b(b-1)n_*} \right) \\ \frac{\partial n_*}{\partial N} &= \frac{bn_*}{b(b+1)N - b(b-1)n_*} \end{aligned}$$

and, more simply

$$\begin{aligned} \frac{\partial}{\partial a} \ell(n_*; \theta) &= (N - n_*)n_*^{-b} \\ \frac{\partial}{\partial b} \ell(n_*; \theta) &= -\log(n_*)(N - n_*)an_*^{-b} \\ \frac{\partial}{\partial c} \ell(n_*; \theta) &= N - n_* \\ \frac{\partial}{\partial k_1} \ell(n_*; \theta) &= n_* \\ \frac{\partial}{\partial N} \ell(n_*; \theta) &= an_*^{-b} + c \end{aligned}$$

A3 Consistency of emulation approach

Theorem 3. *If $\ell(n)$, σ , and $m(n, \Theta)$ are almost surely bounded and $d_i \sim N(l(n_i), \sigma_i^2)$ then for every $n \in \{1, \dots, N\}$, as the multiplicity of n in \mathbf{n} tends to ∞ we have $\mu(n) \rightarrow \ell(n)$ and $\Psi(n) \rightarrow 0$ almost surely with respect to variation in \mathbf{d} .*

Proof. Assume W.L.O.G that $(\mathbf{n}^1)_1 = n$. Since σ is bounded, we have (from equation (12)) $\text{var}((\mathbf{d}^1)_1) = (\sigma^1)_1^2 \rightarrow 0$, so $(\mathbf{d}^1)_1 \rightarrow \ell(n)$ almost surely. We now prove that $k(n, \mathbf{n}^1)[k(\mathbf{n}^1, \mathbf{n}^1) + \text{diag}((\sigma^1)^2)]^{-1} = (1, 0, \dots, 0)$ when $(\sigma^1)_1 = 0$. Now:

$$\begin{aligned} k(n, \mathbf{n}^1)[k(\mathbf{n}^1, \mathbf{n}^1) + \text{diag}((\sigma^1)^2)]^{-1} &= (1, 0, \dots, 0) \\ \Leftrightarrow k(n, \mathbf{n}^1) &= (1, 0, \dots, 0) * k(\mathbf{n}^1, \mathbf{n}^1 + \text{diag}((\sigma^1)^2)) \end{aligned} \quad (39)$$

and $k(n, \mathbf{n}^1) = (1, 0, \dots, 0) * k(\mathbf{n}^1, \mathbf{n}^1 + \text{diag}((\sigma^1)^2)_{-1})$ is true by definition as the first row of $k(\mathbf{n}^1, \mathbf{n}^1) + \text{diag}((\sigma^1)^2)$ is $k(n, \mathbf{n}^1)$. Therefore,

$$\mu(n) = m(n, \Theta) + (1, 0, \dots, 0)(\mathbf{d}^1 - m(\mathbf{n}^1, \Theta)) = m(n, \Theta) + d(n) - m(n, \Theta) = d(n) = \ell(n) \quad (40)$$

almost surely, and

$$\Psi(n) = k(n, n) - (1, 0, \dots, 0)k(\mathbf{n}^1, n) = k(n, n) - k(n, n) = 0 \quad (41)$$

in the limit. □

Corollary 4.1. *Given the conditions of Theorem 3, for every $n \in \{1, \dots, N\}$, as the multiplicity of n in \mathbf{n} tends to ∞ ,*

$$EI(n) \rightarrow 0$$

almost surely with respect to randomness in \mathbf{d}

Proof. From Theorem 3 we have that $\mu(n) \rightarrow \ell(n) < \infty$ and $d_i^1 \rightarrow \ell(n_i^1)$, so therefore in the limit we can state $P_{\mathbf{d}}(-\infty < d^- - \mu(n) \leq 0) = 1$. Indeed, let j be the index such that $n_j^1 = n$. If in the limit $d^- > \mu(n) = d(n)$ then this implies that $d_j^1 < \min_i\{d_i^1\}$ which is a contradiction. Also note from Theorem 3 that $\Psi(n) \rightarrow 0$ and that $\Phi(\cdot) \in (0, 1)$, $\phi(\cdot) \in (0, (2\pi)^{-1/2}]$. As a result the following two scenarios have joint probability 1:

- $d^- - \mu(n) = 0$ in the limit: As $\Phi(\cdot)$, $\phi(\cdot)$ are bounded and $\Psi(n) = 0$ in the limit, we also have $EI(n) = 0$ in the limit.
- $\infty < d^- - \mu(n) < 0$ in the limit: As $\Psi(n) = 0$ in the limit, $\Phi\left(\frac{d^- - \mu(n)}{\sqrt{\Psi(n)}}\right) = 0$ in the limit. As $\phi(\cdot)$ is bounded we have that $EI(n) = 0$ in the limit.

which proves the corollary □

Theorem 4. *If $\ell(n)$, σ , and $m(n, \Theta)$ are almost surely bounded and $d_i \sim N(\ell(n_i), \sigma_i^2)$ then under algorithm 2 with $\tau = 0$, the value $\mu(\tilde{n})$ converges almost surely to $\ell(\tilde{n})$ for every $\tilde{n} \in \{1, \dots, N\}$.*

Proof. Our overall argument is to show that algorithm 2 leads to the multiplicity of \tilde{n} in \mathbf{n} tending to infinity, from which the result follows from Theorem 3.

To do this, we begin with the following two lemmas, the second of which describes the limiting behaviour of $EI(n)$ according to how often n occurs in \mathbf{n} : namely that if the multiplicity of n in \mathbf{n} diverges, the value of $EI(n)$ converges to 0; otherwise, it remains positive. We introduce the index $EI_{\mathbf{n}}(n)$ to indicate the dependence of $EI(n)$ on \mathbf{n} and assume that the function $\ell(n)$ is fixed. For a multiset \mathbf{n}_i , we denote $\text{mult}_{\mathbf{n}_i}(n)$ as the multiplicity of n in \mathbf{n}_i .

Lemma 4.1. *Suppose $m \times m$ matrix A is symmetric. Denote by I^1 the $m \times m$ matrix with $I_{ij}^1 = 1_{i=j=1}$. Let x be a vector of length m and denote by A_x the matrix A with its top row replaced by x . Then for p in any interval containing 0 on which $A + pI^1$ is invertible we have*

$$\frac{\partial}{\partial p} (x^T (A + pI^1)^{-1} x) = -\frac{|A_x|^2}{|A + pI^1|^2} \quad (42)$$

Proof. If $M(p)$ is invertible in a neighbourhood of p we have $\frac{\partial M^{-1}}{\partial p} = -M^{-1} \frac{\partial M}{\partial p} M^{-1}$, and if M is symmetric with dimensions $m \times m$ and first row M_1 , then $M I^1 M = M_1 M_1^T$. Since $(A + pI)$ and A differ only in the top row, we have $\text{adj}(A + pI)_1 = \text{adj}(A)_1$, where $\text{adj}(\cdot)$ indicates the adjugate matrix and \cdot_1 the top row. We now have

$$\begin{aligned} \frac{\partial}{\partial p} (x^T (A + pI^1)^{-1} x) &= -x^T (A + pI^1)^{-1} \frac{\partial (A + pI^1)}{\partial p} (A + pI^1)^{-1} x \\ &= -x^T (A + pI^1)^{-1} I^1 (A + pI^1)^{-1} x \\ &= \frac{x^T \text{adj}(A + pI^1) I^1 \text{adj}(A + pI^1) x}{|A + pI^1|^2} \\ &= -\frac{x^T \text{adj}(A + pI^1)_1 \text{adj}(A + pI^1)_1^T x}{|A + pI^1|^2} \\ &= -\frac{x^T \text{adj}(A)_1 \text{adj}(A)_1^T x}{|A + pI^1|^2} \\ &= -\frac{|A_x|^2}{|A + pI^1|^2} \end{aligned}$$

as required. \square

Lemma 4.2. *Let S_1 and S_2 be disjoint subsets of $[N] = \{1, 2, \dots, N\}$ with $S_1 \cup S_2 = [N]$. For a multiset \mathbf{n} denote*

$$\begin{aligned} q_1(\mathbf{n}) &= \max_{n \in S_1} \text{mult}_{\mathbf{n}}(n) \\ q_2(\mathbf{n}) &= \min_{n \in S_2} \text{mult}_{\mathbf{n}}(n) \end{aligned} \tag{43}$$

Suppose we have infinite sequences \mathbf{n} , \mathbf{d} , $\boldsymbol{\sigma}$, where $\mathbf{d} \sim N(l(\mathbf{n}), \boldsymbol{\sigma}^2)$ and $\boldsymbol{\sigma}^2$ is upper-bounded, and let \mathbf{n}_i , \mathbf{d}_i , $\boldsymbol{\sigma}_i$ denote the (multiset) first i elements of each sequence. Suppose that $q_1(\mathbf{n}_i) \leq m_1$ for all i and $q_2(\mathbf{n}_i) \rightarrow \infty$, and the set $\{k_2(n, \Theta_i) \triangleq k_2(n, \Theta(\mathbf{n}_i, \mathbf{d}_i, \boldsymbol{\sigma}_i)) : n \in 1 \dots N, i \in \mathbb{N}\}$ is almost surely asymptotically bounded. Then for sufficiently large σ_u :

$$\limsup_{i \rightarrow \infty} EI_{\mathbf{n}_i}(n) = \begin{cases} e_n > 0 & \text{if } n \in S_1 \\ 0 & \text{if } n \in S_2 \end{cases} \tag{44}$$

almost surely.

Proof. We will in fact show that even $\liminf EI_{\mathbf{n}_i}(n) > 0$ for $n \in S_1$, but \limsup will suffice for our purposes. We note that

$$EI_{\mathbf{n}_i}(n) > 0 \Leftrightarrow \sqrt{\Psi_{\mathbf{n}_i}(n)} \phi \left(\frac{d_{\mathbf{n}_i}^- - \mu_{\mathbf{n}_i}(n)}{\sqrt{\Psi_{\mathbf{n}_i}(n)}} \right) > (\mu_{\mathbf{n}_i}(n) - d_{\mathbf{n}_i}^-) \Phi \left(\frac{d_{\mathbf{n}_i}^- - \mu_{\mathbf{n}_i}(n)}{\sqrt{\Psi_{\mathbf{n}_i}(n)}} \right) \tag{45}$$

We will show that for all n , we have

$$P \left(-\infty < \liminf_{i \rightarrow \infty} (d_{\mathbf{n}_i}^- - \mu_{\mathbf{n}_i}(n)) \right) = 1 \tag{46}$$

By the argument in theorem 3 and corollary 4.1 we have for $n \in S_2$ that $\lim_{i \rightarrow \infty} \Psi_{\mathbf{n}_i}(n) = 0$, from which both sides of (45) converge to 0. For $n \in S_1$ we will show $\lim_{i \rightarrow \infty} \Psi_{\mathbf{n}_i}(n) > 0$, in which case we may define

$$z_{\mathbf{n}_i}(n) = \frac{\mu_{\mathbf{n}_i}(n) - d_{\mathbf{n}_i}^-}{\sqrt{\Psi_{\mathbf{n}_i}(n)}} \tag{47}$$

from which inequality (45) reduces to

$$\phi(z_{\mathbf{n}_i}(n)) > z_{\mathbf{n}_i}(n) \Phi(-z_{\mathbf{n}_i}(n)) \tag{48}$$

which holds for all $0 \leq z_{\mathbf{n}_i}(n) < -\infty$. Since $z_{\mathbf{n}_i}(n)$ is asymptotically bounded between positive values, the result follows.

Beginning with $d_{\mathbf{n}_i}^-$, we note that $d_{\mathbf{n}_i}^-$ is the minimum of

1. Values of \mathbf{d}_i^1 corresponding to values of \mathbf{n}_i^1 in S_1 ; and
2. Values of \mathbf{d}_i^1 corresponding to values of \mathbf{n}_i^1 in S_2

For sufficiently large s , the sequence $\{n_j = (\mathbf{n})_j : j > s\}$ never contains any $n \in S_1$ again; hence, the minimum of item 1 is determined after finitely many i and its limit is finite. Since $\boldsymbol{\sigma}$ is upper-bounded, all values of \mathbf{d}_i^1 in item 2 converge to finite values in $\{\ell(n) : n \in S_2\}$ almost surely. Hence $d_{\mathbf{n}_i}^-$ converges almost surely to a finite value.

Since $\limsup_{i \rightarrow \infty}$ and $\liminf_{i \rightarrow \infty}$ of $m(n; \Theta(\mathbf{n}_i, \mathbf{d}_i, \boldsymbol{\sigma}_i))$ are almost surely finite, all terms in $\mu(n)$ are asymptotically finite, from which equation (46) follows.

It remains to consider $\Psi_{\mathbf{n}_i}(n)$ for $n \in S_1$. Firstly take $n \in \mathbf{n}^1$ and suppose W.L.O.G that $\mathbf{n}_i^1 = n$. Since $n \in S_1$ we have $\lim_{i \rightarrow \infty} \text{mult}_{\mathbf{n}_i}(n) > 0$ so $\lim_{i \rightarrow \infty} (\boldsymbol{\sigma}_i^1)_1$ exists and is positive. Denoting $\boldsymbol{\sigma}'$ as $\boldsymbol{\sigma}_i^1$ with 0 substituted for the first element, we have

$$\begin{aligned} \frac{\partial}{\partial (\boldsymbol{\sigma}_i^1)_1^2} \Psi_{\mathbf{n}_i}(n) &= \frac{\partial}{\partial (\boldsymbol{\sigma}_i^1)_1^2} (k(n, n) - k(n, \mathbf{n}_i^1)[k(\mathbf{n}_i^1, \mathbf{n}_i^1) + \text{diag}((\boldsymbol{\sigma}_i^1)^2)]^{-1}k(\mathbf{n}_i^1, n)) \\ &= \frac{|k(\mathbf{n}_i^1, \mathbf{n}_i^1) + \text{diag}((\boldsymbol{\sigma}')^2)|^2}{|k(\mathbf{n}_i^1, \mathbf{n}_i^1) + \text{diag}((\boldsymbol{\sigma}_i^1)^2)|^2} > 0 \end{aligned}$$

by lemma 4.1; hence $\Psi_{\mathbf{n}_i}(n)$, considered as a function of $(\boldsymbol{\sigma}_i^1)_1^2$, is increasing. Given that $\lim_{i \rightarrow \infty} (\boldsymbol{\sigma}_i^1)_j$ is 0 for $(\mathbf{n}_i^1)_j \in S_2$ and is positive for $(\mathbf{n}_i^1)_j \in S_1$, we conclude that $\lim_{i \rightarrow \infty} \Psi_{\mathbf{n}_i}(n)$ is positive when $n \in S_1$ and $n \in \mathbf{n}^1$.

If $n \notin \mathbf{n}^1$, so n never occurs in any \mathbf{n}_i , then we firstly note that since $k(n, n) < k(n, m)$ for any $m \neq n$, we have:

$$k(n, n) - k(n, \mathbf{n}_i^1)[k(\mathbf{n}_i^1, \mathbf{n}_i^1)]^{-1}k(\mathbf{n}_i^1, n) > 0 \quad (49)$$

This omits the term $\text{diag}((\boldsymbol{\sigma}_i^1)^2)$ from the expression for $\Psi_{\mathbf{n}_i}(n)$. However, if we denote k'_j the matrix $k(\mathbf{n}_i^1, \mathbf{n}_i^1) + \text{diag}((\boldsymbol{\sigma}_i^1)^2)$ with the j th row replaced by $k(n, \mathbf{n}_i^1)$, we have from lemma 4.1:

$$\frac{\partial}{\partial (\boldsymbol{\sigma}_i^1)_j^2} \Psi_{\mathbf{n}_i}(n) = \frac{|k'_j|^2}{|k(\mathbf{n}_i^1, \mathbf{n}_i^1) + \text{diag}((\boldsymbol{\sigma}_i^1)^2)|^2} > 0$$

for any element $(\boldsymbol{\sigma}_i^1)_j^2$ of $(\boldsymbol{\sigma}_i^1)^2$; hence $\Psi_{\mathbf{n}_i}(n)$ is increasing in any such element and its positivity follows. This completes the proof of the lemma. \square

Now suppose that some $n \in \{1 \dots N\}$ occurs only finitely often in \mathbf{n}^1 . Then there must be some largest set S_1 of such n , with complement $S_2 = \{1 \dots N\} \setminus S_1$. Since every element in S_1 occurs in \mathbf{n}^1 with finite multiplicity there must be some j such that no $n \in S_1$ occurs amongst the values $\{(\mathbf{n}^1)_{j+1}, (\mathbf{n}^1)_{j+2}, \dots\}$. But from lemma 4.2, there will almost surely eventually be some $J > j$ for which some value in $\{EI_{\mathbf{n}_J}(n) : n \in S_1\}$ exceeds all

values in $\{EI_{\mathbf{n}_J}(n) : n \in S_1\}$, and hence $(\mathbf{n}^1)_{J+1} \in S_1$ (as long as τ is sufficiently small), contradicting the choice of j . So the event that an $n \in \{1 \dots N\}$ occurs in \mathbf{n}^1 with finite multiplicity has probability 0. This completes the proof. \square

References

ACOG. Practice advisory on low-dose aspirin and prevention of preeclampsia: Updated recommendations. *American College of Obstetricians and Gynecologists (ACOG)* (2016).

AD, NIV, HOLMES, SARI D., PATEL, JAY, PRITCHARD, GRACIELA, SHUMAN, DEBORAH J., and HALPIN, LINDA. Comparison of EuroSCORE II, original EuroSCORE, and The Society of Thoracic Surgeons risk score in cardiac surgery patients. *The Annals of Thoracic Surgery*, 102(2):573–579 (2016). doi:10.1016/j.athoracsur.2016.01.105.

AKOLEKAR, RANJIT, SYNGELAKI, ARGYRO, POON, LEONA, WRIGHT, DAVID, and NICOLAIDES, KYPROS H. Competing risks model in early screening for preeclampsia by biophysical and biochemical markers. *Fetal diagnosis and therapy*, 33(1):8–15 (2013).

ALAA, AHMED M and VAN DER SCHAAR, MIHAELA. Autoprognosis: Automated clinical prognostic modeling via Bayesian optimization with structured kernel learning. *arXiv preprint arXiv:1802.07207* (2018).

AMARI, SHUN-ICHI. A universal theorem on learning curves. *Neural networks*, 6(2):161–166 (1993).

AMARI, SHUN-ICHI, FUJITA, NAOTAKE, and SHINOMOTO, SHIGERU. Four types of learning curves. *Neural Computation*, 4(4):605–618 (1992).

ANDRIANAKIS, Y and CHALENOR, PG. Parameter estimation for Gaussian process emulators. Technical report, Technical report, Managing Uncertainty in Complex Models (2011).

BARILI, FABIO, PACINI, DAVIDE, CAPO, ANTONIO, RASOVIC, OLIVERA, GROSSI, CLAUDIO, ALAMANNI, FRANCESCO, DI BARTOLOMEO, ROBERTO, and PAROLARI, ALESSANDRO. Does EuroSCORE II perform better than its original versions? A multicentre validation study. *European heart journal*, 34(1):22–29 (2013).

BEN-ISRAEL, DAVID, JACOBS, W BRADLEY, CASHA, STEVE, LANG, STEFAN, RYU, WON HYUNG A, DE LOTBINIERE-BASSETT, MADELEINE, and CADOTTE, DAVID W. The impact of machine learning on patient care: a systematic review. *Artificial intelligence in medicine*, 103:101785 (2020).

BOWER, RICHARD G, GOLDSTEIN, MICHAEL, and VERNON, IAN. Galaxy formation: a Bayesian uncertainty analysis. *Bayesian analysis*, 5(4):619–669 (2010).

BROCHU, ERIC, CORA, VLAD M, and DE FREITAS, NANDO. A tutorial on Bayesian optimization of expensive cost functions, with application to active user modeling and hierarchical reinforcement learning. *arXiv preprint arXiv:1012.2599* (2010).

BULL, ADAM D. Convergence rates of efficient global optimization algorithms. *Journal of Machine Learning Research*, 12(10) (2011).

CHALMERS, JOHN, PULLAN, MARK, FABRI, BRIAN, McSHANE, JAMES, SHAW, MATTHEW, MEDIRATTA, NEERAJ, and POULLIS, MICHAEL. Validation of EuroSCORE II in a modern cohort of patients undergoing cardiac surgery. *European Journal of Cardio-Thoracic Surgery*, 43(4):688–694 (2013).

COLLINS, GARY S, DHIMAN, PAULA, NAVARRO, CONSTANZA L ANDAUR, MA, JI, HOOFT, LOTTY, REITSMA, JOHANNES B, LOGULLO, PATRICIA, BEAM, ANDREW L, PENG, LILY, VAN CALSTER, BEN, ET AL. Protocol for development of a reporting guideline (TRIPOD-AI) and risk of bias tool (PROBAST-AI) for diagnostic and prognostic prediction model studies based on artificial intelligence. *BMJ open*, 11(7):e048008 (2021).

COLLINS, GARY S, REITSMA, JOHANNES B, ALTMAN, DOUGLAS G, and MOONS, KAREL GM. Transparent reporting of a multivariable prediction model for individual prognosis or diagnosis (TRIPOD): The TRIPOD statement. *Circulation*, 131(2):211–219 (2015).

COOK, J. A. and COLLINS, G. S. The rise of big clinical databases. *British Journal of Surgery*, 102(2):e93–e101 (2015). doi:10.1002/bjs.9723.

DRUSVYATSKIY, DMITRIY and XIAO, LIN. Stochastic optimization with decision-dependent distributions. *arXiv preprint arXiv:2011.11173* (2020).

DURAND, ERIC, BORZ, BOGDAN, GODIN, MATTHIEU, TRON, CHRISTOPHE, LITZLER, PIERRE-YVES, BESSOU, JEAN-PAUL, DACHER, JEAN-NICOLAS, BAUER, FABRICE, CRIBIER, ALAIN, and ELTCHANINOFF, HÉLÈNE. Performance analysis of EuroSCORE II compared to the original logistic EuroSCORE and STS scores for predicting 30-day mortality after transcatheter aortic valve replacement. *The American journal of cardiology*, 111(6):891–897 (2013).

FINLAYSON, SAMUEL G, SUBBASWAMY, ADARSH, SINGH, KARANDEEP, BOWERS, JOHN, KUPKE, ANNABEL, ZITTRAIN, JONATHAN, KOHANE, ISAAC S, and SARIA, SUCHI. The clinician and dataset shift in artificial intelligence. *The New England Journal of Medicine*, pages 283–286 (2020).

HIPPISLEY-COX, JULIA, COUPLAND, CAROL, and BRINDLE, PETER. Development and validation of QRISK3 risk prediction algorithms to estimate future risk of cardiovascular disease: prospective cohort study. *BMJ*, 357 (2017).

IZZO, ZACHARY, ZOU, JAMES, and YING, LEXING. How to learn when data gradually reacts to your model. *arXiv preprint arXiv:2112.07042* (2021).

JACOBS, JEFFREY PHILLIP, MAVROUDIS, CONSTANTINE, JACOBS, MARSHALL LEWIS, MARUSZEWSKI, BOHDAN, TCHERVENKOV, CHRISTO I, LACOUR-GAYET, FRANÇOIS G, CLARKE, DAVID ROBINSON, YEH JR, THOMAS, WALTERS III, HENRY L, KUROSAWA, HIROMI, ET AL. What is operative mortality? Defining death in a surgical registry database: a report of the STS Congenital Database Taskforce and the joint EACTS-STS Congenital Database Committee. *The Annals of thoracic surgery*, 81(5):1937–1941 (2006).

KANSAGARA, DEVAN, ENGLANDER, HONORA, SALANITRO, AMANDA, KAGEN, DAVID, THEOBALD, CECELIA, FREEMAN, MICHELE, and KRIPALANI, SUNIL. Risk prediction models for hospital readmission: a systematic review. *Jama*, 306(15):1688–1698 (2011).

KILLEYA, MATTHEW RH. *Thinking inside the box: using derivatives to improve Bayesian black box emulation of computer simulators with application to compact mental models*. Ph.D. thesis, Durham University (2004).

KOOPMAN, RICHELLE J and MAINOUS, AG. Evaluating multivariate risk scores for clinical decision making. *Family Medicine*, 40(6):412 (2008).

LEFEVRE, MICHAEL L. Low-dose aspirin use for the prevention of morbidity and mortality from preeclampsia: Us preventive services task force recommendation statement. *Annals of internal medicine*, 161(11):819–826 (2014).

LENERT, MATTHEW C, MATHENY, MICHAEL E, and WALSH, COLIN G. Prognostic models will be victims of their own success, unless.... *Journal of the American Medical Informatics Association*, 26(12):1645–1650 (2019).

LI, QIANG and WAI, HOI-TO. State dependent performative prediction with stochastic approximation. *arXiv preprint arXiv:2110.00800* (2021).

LILEY, JAMES. Stacking interventions for equitable outcomes. *arXiv preprint arXiv:2110.04163* (2021).

LILEY, JAMES, BOHNER, GERGO, EMERSON, SAMUEL R, MATEEN, BILAL A, BORLAND, KATIE, CARR, DAVID, HEALD, SCOTT, ODURO, SAMUEL D, IRELAND, JILL, MOFFAT, KEITH, PORTEOUS, RACHEL, RIDDELL, STEPHEN, ROGERS, SIMON, CUNNINGHAM, NATHAN, HOLMES, CHRIS, PAYNE, KATRINA, VOLLMER, SEBASTIAN J, VALLEJOS, CATALINA A, and ASLETT, LOUIS JM. Development and assessment of a machine learning tool for predicting emergency admission in Scotland. *medRxiv* (2021a).

LILEY, JAMES, EMERSON, SAMUEL R, MATEEN, BILAL A, VALLEJOS, CATALINA A, ASLETT, LOUIS JM, and VOLLMER, SEBASTIAN J. Model updating after interventions paradoxically introduces bias. *AISTATS proceedings* (2021b).

LOCATELLI, MARCO. Bayesian algorithms for one-dimensional global optimization. *Journal of Global Optimization*, 10(1):57–76 (1997).

LU, JIE, LIU, ANJIN, DONG, FAN, GU, FENG, GAMA, JOAO, and ZHANG, GUANGQUAN. Learning under concept drift: A review. *IEEE Transactions on Knowledge and Data Engineering*, 31(12):2346–2363 (2018).

MC HUTCHON, ANDREW JAMES ET AL. *Nonlinear modelling and control using Gaussian processes*. Ph.D. thesis, Citeseer (2015).

MENDLER-DÜNNER, CELESTINE, PERDOMO, JUAN C, ZRNIC, TIJANA, and HARDT, MORITZ. Stochastic optimization for performative prediction. *arXiv preprint arXiv:2006.06887* (2020).

NASHEF, SAMER AM, ROQUES, FRANÇOIS, SHARPLES, LINDA D, NILSSON, JOHAN, SMITH, CHRISTOPHER, GOLDSSTONE, ANTONY R, and LOCKOWANDT, ULF. EuroSCORE II. *European journal of cardio-thoracic surgery*, 41(4):734–745 (2012).

O'GORMAN, NEIL, WRIGHT, DAVID, POON, LC, ROLNIK, DANIEL L, SYNGELAKI, ARGYRO, DE ALVARADO, MERCEDES, CARBONE, ILMA F, DUTEMEYER, VIVIEN, FOLNA, MADGALENA, FRICK, ALEX, ET AL. Multicenter screening for pre-eclampsia by maternal factors and biomarkers at 11–13 weeks' gestation: comparison with NICE guidelines and ACOG recommendations. *Ultrasound in Obstetrics & Gynecology*, 49(6):756–760 (2017).

O'BRIEN, SEAN M, FENG, LIQI, HE, XIA, XIAN, YING, JACOBS, JEFFREY P, BADHWAR, VINAY, KURLANSKY, PAUL A, FURNARY, ANTHONY P, CLEVELAND JR, JOSEPH C, LOBDELL, KEVIN W, ET AL. The Society of Thoracic Surgeons 2018 adult cardiac surgery risk models: part 2—statistical methods and results. *The Annals of thoracic surgery*, 105(5):1419–1428 (2018).

PERDOMO, JUAN, ZRNIC, TIJANA, MENDLER-DÜNNER, CELESTINE, and HARDT, MORITZ. Performative prediction. In *International Conference on Machine Learning*, pages 7599–7609. PMLR (2020).

ROLNIK, DANIEL L, WRIGHT, DAVID, POON, LCY, SYNGELAKI, ARGYRO, O'GORMAN, NEIL, DE PACO MATALLANA, CATALINA, AKOLEKAR, RANJIT, CICERO, SIMONA, JANGA, DEEPA, SINGH, MANDEEP, ET AL. ASPRE trial: performance of screening for preterm pre-eclampsia. *Ultrasound in obstetrics & gynecology*, 50(4):492–495 (2017a).

ROLNIK, DANIEL L, WRIGHT, DAVID, POON, LIONA C, O'GORMAN, NEIL, SYNGELAKI, ARGYRO, DE PACO MATALLANA, CATALINA, AKOLEKAR, RANJIT, CICERO, SIMONA, JANGA, DEEPA, SINGH, MANDEEP, ET AL. Aspirin versus placebo in pregnancies at high risk for preterm preeclampsia. *New England Journal of Medicine*, 377(7):613–622 (2017b).

RYZHOV, ILYA O. On the convergence rates of expected improvement methods. *Operations Research*, 64(6):1515–1528 (2016).

SHAHIAN, DAVID M, JACOBS, JEFFREY P, BADHWAR, VINAY, KURLANSKY, PAUL A, FURNARY, ANTHONY P, CLEVELAND JR, JOSEPH C, LOBDELL, KEVIN W, VASSILEVA, CHRISTINA, VON BALLMOOS, MORITZ C WYLER, THOURANI, VINOD H, ET AL. The Society of Thoracic Surgeons 2018 adult cardiac surgery risk models: part 1—background, design considerations, and model development. *The Annals of thoracic surgery*, 105(5):1411–1418 (2018).

SPERRIN, MATTHEW, JENKINS, DAVID, MARTIN, GLEN P, and PEEK, NIELS. Explicit causal reasoning is needed to prevent prognostic models being victims of their own success. *Journal of the American Medical Informatics Association*, 26(12):1675–1676 (2019).

STALLARD, NIGEL, MILLER, FRANK, DAY, SIMON, HEE, SIEW WAN, MADAN, JASON, ZOHAR, SARAH, and POSCH, MARTIN. Determination of the optimal sample size for a clinical trial accounting for the population size. *Biometrical Journal*, 59(4):609–625 (2017).

STEIN, MICHAEL L. Interpolation of spatial data: Some theory for kriging (1999).

TOPOL, ERIC J. High-performance medicine: the convergence of human and artificial intelligence. *Nature medicine*, 25(1):44–56 (2019).

TSYMBAL, ALEXEY. The problem of concept drift: definitions and related work. *Computer Science Department, Trinity College Dublin*, 106(2):58 (2004).

USFDA ET AL. Proposed regulatory framework for modifications to artificial intelligence/machine learning (AI/ML)-based software as a medical device (SaMD)-discussion paper (2019). <https://www.fda.gov/files/medical%20devices/published/US-FDA-Artificial-Intelligence-and-Machine-Learning-Discussion-Paper.pdf>.

VAZQUEZ, EMMANUEL and BECT, JULIEN. Convergence properties of the expected improvement algorithm with fixed mean and covariance functions. *Journal of Statistical Planning and inference*, 140(11):3088–3095 (2010).

VERNON, IAN, LIU, JUNLI, GOLDSTEIN, MICHAEL, ROWE, JAMES, TOPPING, JEN, and LINDSEY, KEITH. Bayesian uncertainty analysis for complex systems biology models: emulation, global parameter searches and evaluation of gene functions. *BMC systems biology*, 12(1):1–29 (2018).

VIERING, TOM and LOOG, MARCO. The shape of learning curves: a review. *arXiv preprint arXiv:2103.10948* (2021).

WALLACE, EMMA, STUART, ELLEN, VAUGHAN, NIALL, BENNETT, KATHLEEN, FAHEY, TOM, and SMITH, SUSAN M. Risk prediction models to predict emergency hospital admission in community-dwelling adults: a systematic review. *Medical care*, 52(8):751 (2014).

WILLIAMS, MICHAEL. Risk assessment and management of cardiovascular disease in new zealand. *The New Zealand Medical Journal (Online)*, 116(1185) (2003).

WRIGHT, DAVID, AKOLEKAR, RANJIT, SYNGELAKI, ARGYRO, POON, LEONA CY, and NICOLAIDES, KYPROS H. A competing risks model in early screening for preeclampsia. *Fetal diagnosis and therapy*, 32(3):171–178 (2012).

YANG, JUAN, PEARL, MICHELLE, DELORENZE, GERALD N, ROMERO, ROBERTO, DONG, ZHONG, JELLIFFE-PAWLOWSKI, LAURA, CURRIER, ROBERT, FLESSEL, MONICA, and KHARRAZI, MARTIN. Racial-ethnic differences in midtrimester maternal serum levels of angiogenic and antiangiogenic factors. *American journal of obstetrics and gynecology*, 215(3):359–e1 (2016).

ZLIOBAITE, INDRE. Learning under concept drift: an overview. *arXiv preprint arXiv:1010.4784* (2010).

Optimal sizing of a holdout set for safe predictive model updating

Supplementary material

S1 Emulation of cost function with nugget term

Rather than explaining the variation of values in \mathbf{d} corresponding to a design point in \mathbf{n}^1 as approximation error of a deterministic loss function, we can explain this variation as the result of not including active variables, being the data (X, Y) . Note that as a consequence we are now not emulating a deterministic function $\ell(n)$ as we are not generalising the loss through expectations, we are generalising the loss through omission of the data which generated \mathbf{d} . To clarify this distinction we replace the loss function $\ell(n)$ with the stochastic function $\mathcal{E}(n)$.

Now we may specify variation in \mathbf{d} using a ‘nugget’ term $w(n)$:

$$\mathcal{E}(n) = m(n) + u(n) + w(n) \quad (50)$$

where $m(n)$ and $u(n)$ are as before but now $w(n)$ represents our nugget term, which we again specify as a Gaussian process:

$$w(n) \sim \mathcal{GP}(0, \kappa(n, n')) \quad (51)$$

with

$$\kappa(n, n') = \begin{cases} \kappa(n) & \text{if } n = n' \\ 0 & \text{otherwise} \end{cases} \quad (52)$$

Since there is less variance in risk scores fitted to larger datasets, we expect less variance in $\mathcal{E}(n)$ for larger n , so we specify $\kappa(n)$ as a monotonically decreasing function in n .

The joint distribution between $\mathcal{E}(n)$ and \mathbf{d}^1 is now:

$$\begin{bmatrix} \mathcal{E}(n) \\ \mathbf{d}^1 \end{bmatrix} \sim \mathcal{N} \left(\begin{bmatrix} m(n) \\ m(\mathbf{n}^1) \end{bmatrix}, \begin{bmatrix} k(n, n) + \kappa(n) & k(n, \mathbf{n}^1) \\ k(\mathbf{n}^1, n) & k(\mathbf{n}^1, \mathbf{n}^1) + \text{diag}(\kappa(\mathbf{n}^1)) \end{bmatrix} \right) \quad (53)$$

This then gives our Bayes linear update equations in terms of $\pi_{\mathbf{n}} = \pi(\mathcal{E}(n) | n, \mathbf{n}^1, \mathbf{d}^1)$ as

$$\begin{aligned} \mu(n) &= \mathbb{E}_{\pi_{\mathbf{n}^1}}(\mathcal{E}(n)) \\ &= m(n) + k(n, \mathbf{n}^1)[k(\mathbf{n}^1, \mathbf{n}^1) + \text{diag}(\kappa(\mathbf{n}^1))]^{-1}(\mathbf{d}^1 - m(\mathbf{n}^1)) \end{aligned} \quad (54)$$

$$\begin{aligned} \Psi(n) &= \text{var}_{\pi_{\mathbf{n}^1}}(\mathcal{E}(n)) \\ &= k(n, n) + \kappa(n) - k(n, \mathbf{n}^1)[k(\mathbf{n}^1, \mathbf{n}^1) + \text{diag}(\kappa(\mathbf{n}^1))]^{-1}k(\mathbf{n}^1, n) \end{aligned} \quad (55)$$

Note that this differs only slightly from the emulator constructed in section 4.3, with the main difference being we now attribute uncertainty in the loss values as an inherent behaviour of our emulator and not in the procedure to obtain these loss values. As a result $\kappa(n)$ does not decrease as the multiplicity of elements of \mathbf{n} increases, which represents a major disadvantage to the uncertainty representation in section 4.3.

One may then be sceptical of the benefit of duplicating design points for this method, and whilst it is possible to use this method without duplication (i.e $\mathbf{n} = \mathbf{n}^1$), the consequence of this would be that we are heavily reliant on a singular sample to locate the minimum which could be misleading. Averaging various samples at the same design point mitigates this potential problem, as does replacing d^- with $\mu^- = \min_i\{\mu(\mathbf{n}^1_i)\}$ as detailed in Brochu et al. (2010). Taking the median of samples instead of a weighted mean is more appropriate here as we are not seeking to accurately approximate an expectation, instead we only wish to avoid extreme samples misleading our search for the minimum.

S2 Estimation of parameters for optimal holdout size in ASPRE

S2.1 Estimation of N

As per our assumptions, we presume we are refitting ASPRE to use in a population of 5 million individuals, from which we have approximately 80,000 new pregnancies per year. The incidence of pregnancy per year is now

$$\frac{8 \times 10^4}{5 \times 10^6} = \frac{1}{125} \quad (56)$$

so we have

$$\begin{aligned} N &\approx 5 \times 8 \times 10^4 \\ &= 400000 \end{aligned} \quad (57)$$

with standard error

$$\begin{aligned} SE(N) &\approx 5 \sqrt{5 \times 10^6 \times \frac{1}{125} \left(1 - \frac{1}{125}\right)} \\ &\approx 1500 \end{aligned} \quad (58)$$

S2.2 Estimation of k_1 and k_2

We assume $\pi = 10\% \approx 2707/25797$, the proportion of individuals assigned to the treatment group in Rolnik et al. (2017a) due to having an estimated risk of PRE > 1%.

To estimate k_1 , we considered the study reported in O’Gorman et al. (2017) assessing sensitivity and specificity of NICE and ACOG guidelines in assessing PRE risk. In this study, 8775 individuals were assessed, amongst which 239 developed PRE, for an overall incidence of $239/8875 \approx 0.027$. We estimated the performance of a ‘baseline’ estimator of PRE risk (that is, in the absence of any ASPRE score) by linearly interpolating the points corresponding to ‘ACOG aspirin’, ‘NICE’ and ‘ACOG’ on ROC curves in Figure 1. On this basis, a baseline estimator identifying the 10% of individuals at highest PRE risk (approximately 800) would correspond to the point (x, y) on the interpolated ROC curve with

$$239x + (8775 - 239)y = 0.1 \times 8875 \quad (59)$$

which occurs at roughly a 20% detection (true positive) rate and a 10% false positive rate, close to that of the NICE guidelines.

Since few women in the study were treated with aspirin, we assume that PRE rates in the highest-10% and lowest-10% risk groups assessed by baseline risk (NICE) are untreated risk (that is, if not treated with aspirin). At the inferred true and false positive rates,

we would expect that amongst the 10% of women designated highest-risk by the NICE guidelines, we have a PRE rate of

$$\begin{aligned}\pi_1 &\approx \frac{\text{TPR} \times (\text{Num. PRE})}{\text{Num. positive}} \\ &= \frac{0.2 \times 239}{0.1 \times 8875} \\ &\approx 0.054\end{aligned}\tag{60}$$

and amongst the 90% designated lower risk, a PRE rate of

$$\begin{aligned}\pi_0 &\approx \frac{(1 - \text{TPR}) \times (\text{Num. PRE})}{\text{Num. negative}} \\ &= \frac{0.8 \times 239}{0.9 \times 8875} \\ &\approx 0.024\end{aligned}\tag{61}$$

Given that true positive rates of the NICE guidelines are computed as a fraction with denominator 239, we presume standard errors of π_1 and π_0 of

$$\begin{aligned}SE(\pi_1) &\approx \frac{\sqrt{\pi_1(1 - \pi_1)}}{8875 \times 0.1} \\ &\approx 0.0076 \\ SE(\pi_0) &\approx \frac{\sqrt{\pi_0(1 - \pi_0)}}{8875 \times 0.9} \\ &\approx 0.0017\end{aligned}\tag{62}$$

Now, treating errors in π_0 , π_1 and α as pairwise independent

$$\begin{aligned}k_1 &= \pi_0(1 - \pi) + \pi_1\pi\alpha \\ &\approx 0.0235 \\ SE(k_1) &= SE(\pi_0(1 - \pi) + \pi_1\pi\alpha) \\ &\approx 0.0016\end{aligned}\tag{63}$$

We estimate the population prevalence π_{PRE} of untreated PE as the frequency observed in the original ASPRE data:

$$\pi_{PRE} = \frac{1426}{57974} \approx 2.4\%\tag{64}$$

Note that, although this is approximately equal to π_0 , they are different quantities: π_0 is the population frequency of PRE amongst individuals at the lowest 90% risk by NICE guidelines.

Denoting $\pi_1(n)$ as the untreated risk of PRE in the top 10% of individuals according to an ASPRE score trained on n individuals (and $\pi_0(n)$ correspondingly), we note that it is equal to the sensitivity (or TPR) of the risk score at the level where proportion π of individuals are designated high-risk. Thus for any training set size n

$$\pi_0(n) = \frac{\pi_{PRE} - \pi\pi_1(n)}{1 - \pi} \quad (65)$$

so the average cost to an individual in the intervention set may be expressed in terms of $\pi_1(n)$:

$$\begin{aligned} k_2(n) &= \pi_0(n)(1 - \pi) + \pi_1(n)\pi\alpha \\ &= \pi_{PRE} - \pi\pi_1(n)(1 - \alpha) \end{aligned} \quad (66)$$

S2.3 Implementation

We implemented the complete ASPRE model as described in Rolnik et al. (2017b). We simulated a population of individuals with a similar distribution of ASPRE model covariates. We computed the ASPRE scores for our simulated individuals, and found a linear transformation of these scores such that, should the scores exactly specify the probability of PRE, the expected population prevalence and sensitivity of the score would match those reported in Rolnik et al. (2017a): prevalence π_{PRE} , and sensitivity amongst 10% highest scores: 12.3%. We then simulated PRE incidence according to these transformed scores.

We found that a generalised linear model with logistic link performed almost as well as the ASPRE score on our simulated data, so we used this model type to estimate the learning curve in the interests of simplicity.

To choose values \mathbf{n} and \mathbf{k}_2/\mathbf{d} , we initially chose a set \mathbf{n} of 20 random values from [500, 30000]. For each size n in \mathbf{n} , we took a random sample of our data of size n , fitted a logistic model to that sample, and estimated corresponding expected costs per individual \mathbf{k}_2 as above. We fitted values $\theta = \theta(\mathbf{n}, \mathbf{k}_2) = (a, b, c)$ parametrising k_2 as the maximum-likelihood estimator of θ under the model

$$(\mathbf{k}_2)_i \sim N(k_2((\mathbf{n})_i, \theta), \sigma^2) \sim N(a(\mathbf{n})_i^{-b} + c, \sigma^2) \quad (67)$$

for a fixed values σ , noting that the estimate of θ is independent of σ . For the parametric algorithm, we then set all values of σ to the same value, chosen empirically as the sample variance of

$$\mathbf{k}_2 - k_2(\mathbf{n}, \theta(\mathbf{n}, \mathbf{k}_2)) \quad (68)$$

For the emulation algorithm, we set values \mathbf{d} as

$$\mathbf{d}_i = k_1(\mathbf{n})_i + (\mathbf{k}_2)_i(N - (\mathbf{n})_i) \quad (69)$$

transforming values σ correspondingly for use in the emulation algorithm. We then sequentially chose 100 additional values \mathbf{n} using both algorithm 1 and 2, setting σ as the

same value found in (68). After choosing the 120 values of \mathbf{n} using algorithm 1, we re-estimated \mathbf{k}_2/\mathbf{d} for each of these values before estimating the OHS and confidence interval to avoid any potential regression-to-the mean effects from choosing next-values-of- n so as to minimise estimated confidence interval width.

Our complete pipeline is available at https://github.com/jamesliley/OptHoldoutSize_pipelines, and a comprehensive vignette is included in our R package `OptHoldoutSize` on CRAN and at <https://github.com/jamesliley/OptHoldoutSize>.

S3 Supplementary figures

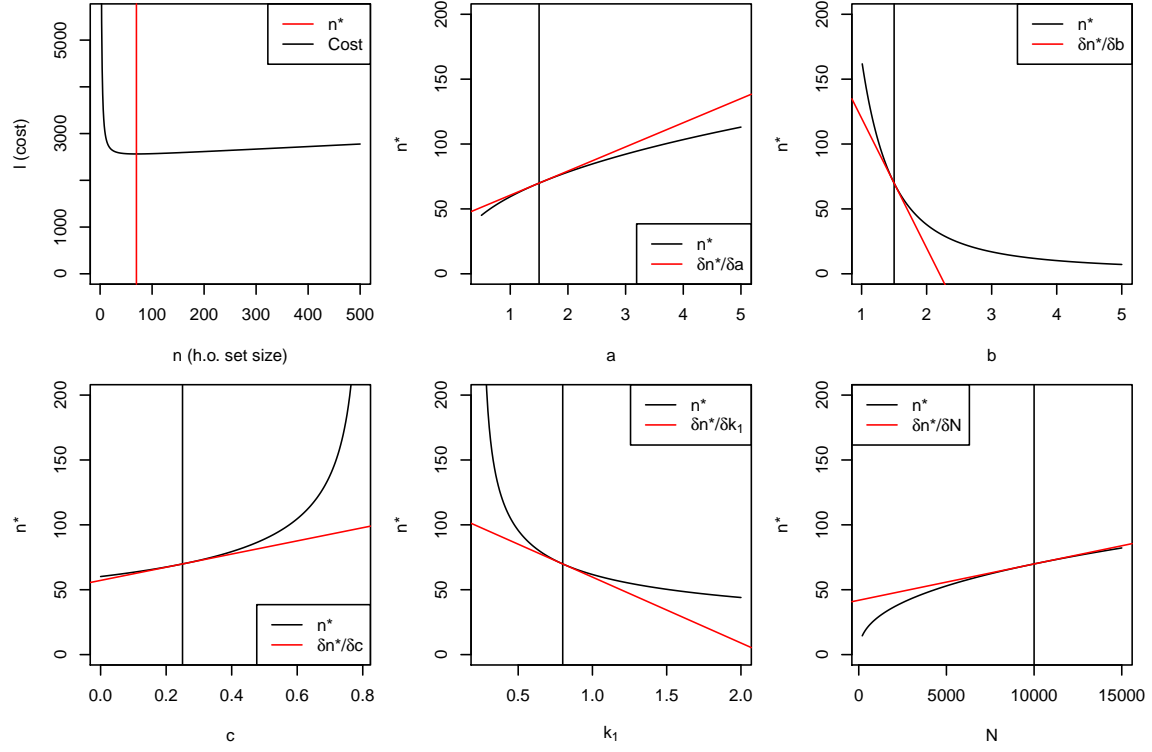


Figure 7: Dependence of optimal holdout set size on parameters of estimated learning curve (a, b, c , with $k_2(n; a, b, c) = an^{-b} + c$), cost in intervention set k_1 , and total number of samples N . Figures show change in optimal holdout set size n_* while varying one parameter and holding others constant at $(a, b, c) = (\frac{3}{2}, \frac{3}{2}, \frac{1}{4})$, $k_1 = \frac{4}{5}$, $N = 10^4$.

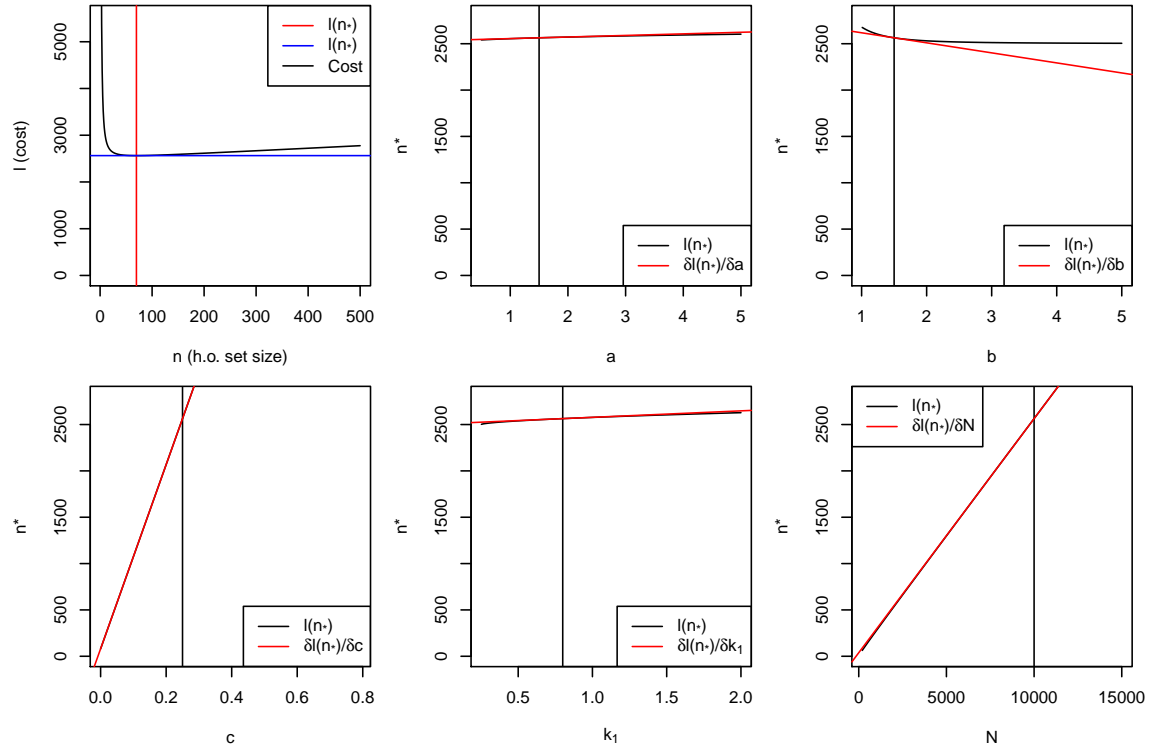


Figure 8: Dependence of minimum total cost on parameters of estimated learning curve (a, b, c , with $k_2(n; a, b, c) = an^{-b} + c$), cost in intervention set k_1 , and total number of samples N . Figures show change in minimal cost $\ell(n_*)$ while varying one parameter and holding others constant at $(a, b, c) = (\frac{3}{2}, \frac{3}{2}, \frac{1}{4})$, $k_1 = \frac{4}{5}$, $N = 10^4$.

References

BROCHU, ERIC, CORA, VLAD M, and DE FREITAS, NANDO. A tutorial on Bayesian optimization of expensive cost functions, with application to active user modeling and hierarchical reinforcement learning. *arXiv preprint arXiv:1012.2599* (2010).

O'GORMAN, NEIL, WRIGHT, DAVID, POON, LC, ROLNIK, DANIEL L, SYNGELAKI, ARGYRO, DE ALVARADO, MERCEDES, CARBONE, ILMA F, DUTEMEYER, VIVIEN, FIOLNA, MADGALENA, FRICK, ALEX, ET AL. Multicenter screening for pre-eclampsia by maternal factors and biomarkers at 11–13 weeks' gestation: comparison with NICE guidelines and ACOG recommendations. *Ultrasound in Obstetrics & Gynecology*, 49(6):756–760 (2017).

ROLNIK, DANIEL L, WRIGHT, DAVID, POON, LCY, SYNGELAKI, ARGYRO, O'GORMAN, NEIL, DE PACO MATALLANA, CATALINA, AKOLEKAR, RANJIT, CICERO, SIMONA, JANGA, DEEPA, SINGH, MANDEEP, ET AL. ASPRE trial: performance of screening for preterm pre-eclampsia. *Ultrasound in obstetrics & gynecology*, 50(4):492–495 (2017a).

ROLNIK, DANIEL L, WRIGHT, DAVID, POON, LIONA C, O'GORMAN, NEIL, SYNGELAKI, ARGYRO, DE PACO MATALLANA, CATALINA, AKOLEKAR, RANJIT, CICERO, SIMONA, JANGA, DEEPA, SINGH, MANDEEP, ET AL. Aspirin versus placebo in pregnancies at high risk for preterm preeclampsia. *New England Journal of Medicine*, 377(7):613–622 (2017b).